RESEARCH ARTICLE



Zinc localization and speciation in rice grain under variable soil zinc deficiency

Yating Shen® · Elizabeth Wiita · Athena A. Nghiem® · Jingyu Liu® · Ezazul Haque® · Rachel N. Austin · Chheng Y. Seng · Kongkea Phan® · Yan Zheng® · Benjamin C. Bostick®

Received: 7 December 2022 / Accepted: 21 June 2023 / Published online: 14 July 2023 © The Author(s), under exclusive licence to Springer Nature Switzerland AG 2023

Abstract

Background and aims Rice accounts for around 20% of the calories consumed by humans. Essential nutrients like zinc (Zn) are crucial for rice growth and for populations relying on rice as a staple food. No well-established study method exists. As a result, we a lack a clear picture of the chemical forms of zinc in rice grain. Furthermore, we do not understand the effects of widespread and variable zinc deficiency in

Responsible Editor: Ismail Cakmak.

Supplementary Information The online version contains supplementary material available at https://doi.org/10.1007/s11104-023-06140-1.

Y. Shen · E. Wiita · A. A. Nghiem · Y. Zheng · B. C. Bostick (\boxtimes)

Lamont-Doherty Earth Observatory of Columbia University, 61 Route 9W, Palisades, New York, NY 10964, USA

e-mail: bostick@ldeo.columbia.edu

Y. Sher

National Research Center for Geo-Analysis (NRCGA), Beijing 100037, China

Y. Shen

Key Laboratory of Eco-Geochemistry, Ministry of Natural Resources of China, Beijing 100037, China

E. Wiita · R. N. Austin Department of Chemistry, Barnard College, New York, NY 10027, USA soils on the Zn speciation, and to a lesser extent, its concentration, in grain.

Methods The composition and Zn speciation of Cambodian rice grain is analyzed using synchrotron-based microprobe X-ray fluorescence (μ-XRF) and extended X-ray absorption fine-structure spectroscopy (EXAFS). We developed a method to quantify Zn species in different complexes based on the coordination numbers of Zn to oxygen and sulfur at characteristic bond lengths.

Results Zn levels in brown rice grain ranged between 15–30 mg kg⁻¹ and were not correlated to Zn availability in soils. 72%-90% of Zn in rice grains is present as Zn-phytate, generally not bioavailable, while smaller quantities of Zn are bound as labile

J. Liu · Y. Zheng

State Environmental Protection Key Laboratory of Integrated Surface Water-Groundwater Pollution Control, School of Environmental Science and Engineering, Southern University of Science and Technology, Shenzhen 518055, China

E. Hague

IDGP in Human Toxicology and Department of Occupational and Environmental Health, University of Iowa, Iowa City, IA 52242, USA

C. Y. Seng · K. Phan
Department of Food Chemistry, Faculty of Science
and Technology, International University,
Phnom Penh 12101, Cambodia



nicotianamine complexes, Zn minerals like $ZnCO_3$ or thiols.

Conclusion Zn speciation in rice grain is affected by Zn deficiency more than previously recognized. A majority of Zn was bound in phytate complexes in rice grain. Zinc phytate complexes were found in higher concentrations and also in higher proportions, in Zn-deficient soils, consistent with increased phytate production under Zn deficiency. Phytates are generally not bioavailable to humans, so low soil Zn fertility may not only impact grain yields, but also decrease the fraction of grain Zn bioavailable to human consumers. The potential impact of abundant Zn-phytate in environments deficient in Zn on human bioavailability and Zn deficiency requires additional research.

 $\begin{tabular}{ll} \textbf{Keywords} & Zn \ deficiency \cdot Bioavailability \cdot \\ Bioaccessibility \cdot Micro-XRF \cdot Zn \ EXAFS \cdot Phytate \\ Zn \end{tabular}$

Introduction

Malnutrition and micronutrient deficiencies are responsible for 3 million child deaths each year (Prentice et al. 2008). In many parts of the world, poor dietary quality and micronutrient deficiencies are more prevalent problems than inadequate energy intake (Stewart et al. 2010). Rice is the most important staple food crop for more than half of the world's population. Over 3.5 billion people depend on rice for more than 20% of the world's daily caloric intake (Seck et al. 2012). Soil nutrient status affects the yield and nutrient content of the rice, and thus is a critical factor affecting food security and nutrition (Brown et al. 2004). One of the most widespread agronomic limits on rice production is the zinc (Zn) nutrient status in soils (Cakmak and Kutman 2018), which in turn can affect Zn content in rice and its bioaccessibility. Human Zn malnutrition is often tied to significant rice consumption (Pfeiffer and McClafferty 2007), leading to stunting in children, susceptibility to infectious diseases, iron deficiency anemia, and reduced birth outcome in pregnant women (Prasad 2014; Graham et al. 2012). About 1.3 billion people are at risk of Zn deficiencies globally (Wessells and Brown 2012).

Zn deficiency in soils is widespread globally (Bansal et al. 1990; Cakmak et al. 1996). The Food and Agriculture Organization (FAO) estimates that 30% of the agricultural soils of the world are Zn deficient (Sillanpää 1982). Soils for rice cultivation are disproportionately at risk of being Zn deficient (Alloway 2009; Dobermann and Fairhurst 2000). Zn deficiency in rice plants causes leaf bronzing at the early growth stages, poor tillering, reduced growth, delayed maturity, and significant yield loss (Dobermann and Fairhurst 2000; Neue et al. 1998). This deficiency is prevalent in part because only a small fraction (a few percent) of soil Zn is available to plants (termed phytoavailable). Paddy soil Zn deficiency commonly results from precipitation as insoluble sulfides, or adsorption of Zn to soil organic carbon and pedogenic oxides, which decrease dissolved Zn levels (Impa and Johnson-Beebout 2012; Gao et al. 2012). Long-term cultivation, widespread in areas of rice production, can also decrease bioavailable Zn pools enough to limit growth (Jones et al. 2013). For example, > 20 kg ha⁻¹ of Zn can be stripped from soils under cultivation in only 100 years, representing much of bioavailable Zn in agricultural landscapes that generally contain < 250 kg total Zn per ha (EA 2007). Zn deficiency in soil not only constrains yields, but also can affect the Zn content of the crop. For example, Zn content in wheat decreases by as much as twofold in Zn-limited environments (Joshi et al. 2010); however, its effect on Zn levels and speciation in rice remains unclear.

Decreased yields and declining nutritional value due to Zn deficiency can have significant implications for people who consume rice. Human Zn deficiency resulting from rice consumption can arise not only from the abundance of rice in their diet, but also differences between the total Zn concentration and the portion with potential for dissolution and biological uptake. The chemical form, or speciation, of Zn is a critical factor affecting its bioaccessibility (the amount of Zn that can be solubilized) and, in turn, its bioavailability (the amount of Zn that is taken up by the plant or human). Although Zn exists as Zn²⁺ in the environment, it forms a variety of organic complexes with S, O, and N-containing ligands (Thomas et al. 2019), as well as many inorganic solids and adsorbed complexes with widely varying bioacces-Myo-inositol-1,2,3,4,5,6-hexakisphosphate, also known as phytic acid (PA) or phytate (PA's



conjugate base), is the primary storage compound for phosphorus (P) in grains. It represents as much as 1.5% of the rice grain mass, and accounts for up to 80% of the total seed phosphorus in rice. Phytate is a potent metal chelator abundant in cereals that can complex Zn and other metals (Liu et al. 2007; Ravindran et al. 1994). Phytate and its Zn complexes are largely insoluble even in acidic conditions, and thus are generally not bioavailable (Bohn et al. 2008). Furthermore, phytate complexes are not bioavailable to humans and other organisms lacking intestinal phytase enzymes to break down phytate (Sandberg and Andersson 1988). For example, only ~3% of Zn in wheat is bioavailable to humans because of phytate complexation (Lemmens et al. 2018). Other Zn chelates appear to be much more bioavailable (Clemens 2014), e.g., Zn-nicotianamine (NA) or chelates binding to other low molecular weight ligands (Eagling et al. 2014). Differentiating these and other complexes are thus key to understand the connection between grain Zn content and its nutritional value.

Although it is clear that reliably characterizing and quantifying the Zn speciation of rice is important, doing so has proven to be challenging. This in part is because Zn is found as a divalent cation, Zn²⁺, in nearly all environments, but that cation can be coordinated to many different ligands. Conventional analytical methods extract Zn²⁺, removing the chemical information about how Zn is complexed within the grain. Energy-dispersive X-ray fluorescence (XRF) spectroscopy is useful to determine trace Zn concentrations in plants (e.g., Rotich et al. 2023). This technique can be performed in situ, at the microscale (µ-XRF) using an X-ray microprobe (e.g., Guilherme Buzanich 2022) and combined with X-ray absorption spectroscopy (XAS) at the same scale (Ketenoglu 2022; Guilherme Buzanich 2022) to measure the distribution and speciation of Zn within plant materials, even at the low concentrations observed in rice. X-ray microtomography on X-ray microprobes can also be used to study element distributions in three dimensions within tissues (Machado et al. 2023), and combined with Zn XANES to learn about speciation (Fanselow et al. 2022). While XAS (Sarret et al. 2002) and μ -XRF has been applied several times in soils and other environmental systems (Castillo-Michel et al. 2017; Grafe et al. 2014; Takahashi et al. 2009), its use for Zn speciation in rice is relatively limited, and in particular, has usually been performed with a very limited number of samples. Consequently, we know relatively little about the Zn speciation in grains grown under typical environmental conditions.

In this study, a combination of μ-XRF and wholegrain XAS is applied to characterize Zn speciation in rice grain from Cambodia grown rice under variable Zn deficiency in soils. Cambodia is an ideal location for this study because of its widespread low soil nutrition conditions (Blair and Blair 2014) and widespread nutritional deficiencies of the population. Synchrotronbased µ-XRF is used to study the localization of Zn within rice grain. Extended X-ray absorption fine structure (EXAFS) spectroscopy is used to determine changes in Zn speciation within rice grains as a function of estimated levels of Zn deficiency. This approach identifies and quantifies the relative proportion of different Zn species based on the local structure of Zn determined from EXAFS (e.g., Bostick et al. 2001; Newville 2001) rather than conventional linear combination fits, which would require prior knowledge of specific components in the rice and their spectra. Results indicate that Zn complexation to phytate in rice grains is extensive and increases with increasing Zn deficiency. Our results also illustrate the effect of growth conditions on Zn concentration and speciation in rice grains, and presumably on the bioavailability of rice Zn concentrations to humans.

Materials & methods

Rice sample collection and handling

Rice samples used in this study were collected in Cambodia directly from subsistence farmers following harvest. All sites were collected from lowland soil paddies. Sampling sites included 16 locations from five provinces of Cambodia located at the west side of the Mekong River north and northeast of Phnom Penh (Fig. S1). These five provinces were chosen because they encompassed a region with a broad spectrum of growth conditions (Ahmed et al. 2011) and rice chemical compositions (Phan et al. 2014; Seyfferth et al. 2014). All samples were collected during field sampling trips in November 2018 or January 2019. Samples collected in November 2018 were grown in the prior year's growing season (Summer 2017 to late 2017/early 2018) which were harvested between Dec. 2017 and March 2018 and



stored until we collected, while samples were collected in January 2019 when a harvest was underway in many areas. Specific sampling sites were chosen by selecting farms within each region and interviewing the farmers at that location. Sites were only included if farmers grew the rice, had it available (usually stored in their home), and knew the precise location where that rice was grown so that a paired soil sample could be taken from the same field. This selection process maximized the number of sampled rice varieties, soil types and fertilities, and environmental conditions. As is typical in Cambodia, all samples were obtained from rainfed paddy fields rather than fields using groundwater irrigation. Although this study did not measure inundation, it is likely that the extent and duration of flooding conditions varied considerably across the sampling sites depending on rainfall, the availability of floodwaters to contribute to the paddy, and other factors.

Rice samples analyzed in this study were grown following traditional rice cultivation practice using transplanted seedlings grown from personal stocks of local rice varieties. In most cases, this meant that rice was grown in rain-fed agricultural settings with little or no fertilizer of any kind (with very limited Zn concentrations in the soil, as shown in Fig. S1), and, to the best of our knowledge, no Zn fertilizer or seed treatments. The total amount of all kinds of fertilizer used in Cambodia averages 9 kg ha⁻¹ y⁻¹, at rates 20-100 times lower than those of neighboring countries (GRiSP et al. 2013). Interviews during sample collection indicates that all of the fields in this study have similarly low fertilizer applications rates, and that most of the ferilizers that are applied are added as manure or as 20-20-20 N-P-K mixes.

All whole rice samples were air-dried, brown rice grains and husks were separated with a small rice polishing machine designed for laboratory-scale work (Nongao, NA-JCB). Polishing small masses of sample can inadvertently remove the bran and considerable flour. To preserve the outer portion of the grain and minimize the flour/bran loss, 3–5 g samples were added in the grinding groove, and polished for only 10 s, after which time, the husk-free grains were picked out with a tweezer. The remaining grains with husk were polished again for another 4 s, and husk-free grains were again removed with tweezers. This was repeated approximately three more times until all

grains were separated from their husks. The separated rice grain was then powdered for subsequent analysis with a clean coffee grinder, reserving some whole grains for microprobe studies or other uses.

Market-purchased rice samples were also analyzed for comparison. These rice grain samples were purchased from a supermarket in the U.S. and were classified by their rice type and country of origin. (Market 2: black rice from China, Market 3: sweet white rice from Thailand, Market 9: red cargo rice from Thailand). These rice grain samples were previously husked and washed before the sale and were used as is following grinding. While they are not labeled as brown or white rice except in one case, it is likely that all are at least milled using a milling machine and thus likely to have some of the aleurone and embryo removed.

Soil sampling

Because these Cambodian rice samples were grown in known field locations, it is possible to examine the soil growth conditions that may have influenced the quantity and speciation of Zn taken up and incorporated into the grain. Composite soil samples of rice paddy soils were collected at the same time as rice samples were collected. Although not collected during the growing season, there was no Zn fertilizer applied to any field, so this soil sample is broadly representative of Zn levels during the previous growing season. Soil samples with a depth of 0-20 cm were collected from each paired field by selecting a random location in the field using a stone toss, and five soil samples were collected from that location and four others 1 m to the north, south, east, and west of that random location (approximate mass 1–1.5 kg wet soil in aggregate). This composite was further homogenized by hand following collection in the laboratory in Cambodia, air-dried, and then it was subsampled into 50-100 g samples, one of which was used in this study. Subsamples were stored at 4 °C in plastic Ziploc slider bags prior to analysis by XRF for composition and other measurements. A Thermo Fisher field-portable XRF analyzer (Model-Niton XL3t Ultra, Tewksbury MA, USA) was used to determine soil concentrations of P, S, Zn, K, Ca, Mn, Fe, Cu, and other metals (See XRF analysis quality control in supporting information, Table S1).

One method of assessing soil Zn nutrient status is to measure the concentration of Zn extracted from soil



using 0.005 M DTPA (diethylenetriaminepentaacetic acid), 0.1 M triethanolamine, and 0.01 M CaCl₂ at pH 7.3 (Johnson-Beebout et al. 2009). This extraction was used on air-dried soil samples following collection. Soil extracts were diluted and measured by inductively coupled plasma mass spectrometer (ICP-MS) using a Thermo Element2 instrument at Lamont-Doherty Earth Observatory at Columbia University. The method had a detection limit of < 0.1 mg Zn/kg after accounting for dilutions.

Rice digestions and elemental analysis

0.20 g rice grain powders were weighed and predigested with 5 mL concentrated HNO3 (Optimagrade) for 24 h, then digested on a hot plate at 90 °C until salt crystal began to form. Then samples were dissolved with 19.5 mL deionized water and 0.5 mL concentrated HNO₃, diluted and the resulting solution was analyzed with ICP-MS using a Ge internal standard as previously described (Cheng et al. 2004). A rice standard reference material, NIST 1568b, was also digested and analyzed to determine the efficiency and accuracy of the procedure. Results were reproducible, and the recovery of Zn, S, P, Fe, Ca, Ba, Na, Mg, K, Mn, Sr, Mo, and Cu ranged from 90 to 105%. Reported concentrations and errors represent means and standard deviations from triplicate extractions and analyses. SPSS was used for statistical comparisons using independent two-sample t-tests (twotail, p < 0.05). Similar statistical methods were also applied to soil composition.

Micro-XRF spectroscopy

 μ -XRF analysis provides information about the spatial distribution of Zn and other elements within the rice grain. μ -XRF data were collected at Stanford Synchrotron Radiation Laboratory (SSRL) on beamline 2–3 using a Si(111) monochromator in continuous scanning mode and 250 ms integration times. This beamline uses Kirkpatrick-Baez mirrors to achieve a nominal beam size of 2 μm×2 μm. One of the whole rice grain samples (KPC-119–3) was polished into a thin slice manually to get a ~1 mm-thick section for μ -XRF analysis. The grain slice was fixed on the Kapton tape. A monochromatic X-ray beam with a photon energy of 12.0 keV was used to excite the sample. The XRF map was obtained by measuring

XRF spectra with a Vortex silicon drift detector (SDD) while continuously rastering the incident beam over the sample using a 3-um step size in both the x and y directions. Elemental abundance for each element was estimated for each point by binning photon energies into regions of interest (ROI, the counts attributed to fluorescence by a specific element), and integrating the number of photons within each ROI. The incident and transmitted X-ray intensity (reported as I₀ and I₁ respectively) are measured using ionization detectors before and after the sample. Measuring I₀ and I₁ allows us to account for the effect of variable incident flux on ROI counts, and to measure sample absorption, $A = log(I_0/I_1)$. XRF microprobe data was processed with Sam's Microprobe Analysis Kit (SMAK) (Mayhew et al. 2011) to correct for sample thickness and incident intensity, and to isolate specific parts of the grain in the images as described in the Supporting Information.

EXAFS spectroscopy

EXAFS spectra were collected at SSRL on beamline 4-1 using a Si (220) double-crystal monochromator with an unfocused beam detuned approximately 50% to reject higher-order harmonic frequencies. An aliquot of each rice powder sample was sealed in Kapton tape, and analyzed in fluorescence mode. Spectra were collected at the Zn K-edge (9659 eV, range from 9430 eV to 10218.5 eV, 0.3 eV spacing at the edge). The energy was calibrated by setting the edge position (first-derivative) of Zn metal to 9659.0 eV. Sample fluorescence was monitored with a 32-element Ge detector (Cramer et al. 1988) oriented 45 degrees off the sample and orthogonal to the incident radiation. Incident and transmitted intensities were measured with 15 cm N₂-filled ionization chambers. For each sample, duplicate EXAFS scans were measured to establish that the Zn coordination was stable in the X-ray beam, and these spectra were averaged for subsequent analysis.

Quantitative EXAFS analysis based on local coordination environment

Model compounds are useful to constrain the interatomic distances and coordination numbers of Zn atoms of Zn bound in rice, including for each shell. There are three distance bonding environments



that are expected to dominate Zn speciation in rice (Table 1): (1) Zn phytate (Bohn et al. 2008) containing short (1.95 Å) tetrahedral Zn–O bonds, (2) Zn-NA (Eagling et al. 2014) or mineral forms of Zn containing longer (2.11 Å) octahedral Zn-O bonding (Bostick et al. 2001), and (3) Zn bound in protein and thiols containing very long (2.34 Å) Zn–S bonds (Persson et al. 2016). These three distinct Zn-O/S distances are easily differentiated based on EXAFS spectroscopy. The second shells are also useful in fitting not only in part because Zn phytate has a unique second shell (Zn-P), but also to differentiate mineral forms of Zn (which contain Zn-metal second-shells) from both Zn-phytate (with Zn-P second-shells) and other organics (with usually indistinct Zn-C coordination in the second shell).

EXAFS spectra were processed using SIXPack (Webb 2005) as follows: EXAFS scans of each sample or reference compound were averaged,

normalized with linear pre-edge and quadratic postedge functions, and then converted to chi functions for EXAFS spectroscopy using a binding energy (E₀) of 9663.5 eV. The $\chi(k)$ spectrum was then weighted by k³ to provide an equal amplitude throughout the entire k-range. The local coordination environment of Zn, including the type (Z), coordination number (CN), distance (R), and the Debye–Waller factor (σ^2) of neighboring atoms, was then determined by fitting the experimental spectrum using Feff 7.0-determined theoretical phase and amplitude functions (Zabinsky et al. 1995; Deleon et al. 1991) and an amplitude correction factor of 0.9. The fit binding energy (E₀) was typically within 3 eV of its initial value. Shell fitting was completed in k-space; however, Fourier-transformed and filtered spectra also were used to examine individual shells in detail. These spectra were obtained by Fourier-transforming k^3 -weighted $\chi(k)$ spectrum

Table 1 The local structures of Zn in various model compounds based on crystallography (XTL) or X-ray absorption spectroscopy (XAS) measurements

Compound	Atom	Coordination number		Distance (A	Å)	Source				
		XTL	XAS	XTL	$XAS \pm \sigma^2$	XTL	XAS			
ZnO	Zn-O	4	5.03	1.96	2.01 ± 0.004	(Abrahams and Bernstein	(Bostick et al. 2001)			
	Zn-Zn	12	10.6	3.21	3.19 ± 0.006	1969)				
$Zn(OH)_2$	Zn-O	6	6	1.87-2.06	1.95-2.08	(Christensen 1969)	(O'day et al. 1998)			
	Zn-Zn	2	-	3.29	-					
	Zn-Zn	2	-	3.50	-					
$ZnCO_3$	Zn-O	6	5.87	2.11	2.11 ± 0.005	(Effenberger et al. 1981)	(Bostick et al. 2001)			
	Zn-C	6	-	2.98	-					
	Zn-Zn	6	6.12	3.67	3.69 ± 0.004					
Zn-nicotianamine (Zn-	Zn-O	-	6.3	-	2.093 ± 0.014		(Trampczynska et al. 2010)			
NA)	Zn-C	-	3.5	-	2.917 ± 0.013					
Zn-thiolate in protein	Zn-S	-	4	-	2.30		(Clark-Baldwin et al. 1998)			
ZnS	Zn-S	4	3.83	2.34	2.35 ± 0.005	(Kisi and Elcombe 1989)	(Bostick et al. 2001)			
	Zn-Zn	12	8.06	3.82	3.85 ± 0.008					
Zn phytate	Zn-O	-	4.0	-	1.98 ± 0.006		(Sarret et al. 2001)			
	Zn-P	-	0.9	-	3.12 ± 0.008					
	Zn-P	-	0.6	-	3.60 ± 0.012					
$Zn_3(PO_4)_2 \cdot 2H_2O$	Zn-O	-	4.0	-	-		(Sarret et al. 2001)			
	Zn-P	-	2.0	-	3.16 ± 0.008					
	Zn-P	-	2.0	-	3.60 ± 0.012					

^{(-):} Not available

 $^{(\}sigma^2)$: Debye–Waller factor in \mathring{A}^2



without smoothing to produce a radial structure function (RSF), which could be sectioned to isolate the contributions of each atomic shell, and these individual shells back-transformed into isolated $\chi(k)$ functions representing each shell.

Although four shells (tetrahedral and octahedral Zn-O, tetrahedral Zn-S, and Zn-P) are potentially present in each EXAFS spectrum, it is not possible to fit the distance, coordination number, and disorder of each shell independently because such fitting would require too many variables for fits to be stable and produce meaningful coordination numbers due to the strong correlation between coordination numbers and the Debye-Waller factor. As a result, the coordination numbers for the four resulting shells (tetrahedral and octahedral Zn-O, tetrahedral Zn-S, and Zn-P) were fit by fixing the interatomic distance and σ^2 of each path based on literature values. For Zn phytate, σ^2 is fixed at 0.006 for tetrahedral Zn-O shells, while σ^2 is 0.005 for octahedral Zn-O in Zn-NA/mineral, and 0.006 for tetrahedral Zn-S (See path fitting data in excel file).

The fraction of each of the three Zn species was determined using the fit coordination numbers for the first shell (primary coordination shell) based on the decrease in their coordination numbers relative to that of the pure material, as described previously (Bostick et al. 2001). These fractions of each of the species $(f_i) f_{\text{Zn phytate}}, f_{\text{Zn NA/mineral}}, \text{ and } f_{\text{Zn Thiol/protein}}$ were determined with the ratio of the fit coordination number (CN_i) to the pure model compound:

$$f_{ZnPhytate} = \frac{CN_{Zn-O,tet}}{4}$$

$$f_{ZnNA/mineral} = \frac{CN_{Zn-O,oct}}{4}$$

$$f_{ZnThiol/Protein} = \frac{CN_{Zn-S,tet}}{4}$$

The fractions ideally sum to 1, but in practice seldom do because coordination numbers are correlated to disorder, which can vary somewhat from ideal. To account for this variation, we apply a normalization factor N that accounts for a total of unnormalized fractions:

$$N = \frac{CN_{Zn-O,tet}}{4} + \frac{CN_{Zn-O,oct}}{6} + \frac{CN_{Zn-S,tet}}{4}$$

This normalization factor N can then be used to normalize each fraction:

$$f_{Znphytate,norm} = \left(\frac{CN_{Zn-O,tet}}{4}\right) \frac{1}{N}$$

$$f_{ZnNA/Mineral,norm} = \left(\frac{CN_{Zn-O,oct}}{6}\right) \frac{1}{N}$$

$$f_{ZnThiol/Protein,norm} = \left(\frac{CN_{Zn-S,tet}}{4}\right) \frac{1}{N}$$

The same analysis can be applied to normalize the uncertainty in coordination number, which depends on data quality, number of variables, fit range and interval. Typical values of N were between 0.8 and 1.1, with fractional uncertainties of 8–14%.

It is important to note that this method of quantifying Zn speciation is different than the other methods that are commonly applied, most of which use linear combination fitting of experimental spectra with a series of reference spectra of pure compounds of known structure. This is necessary because linear combination fitting requires the references to be identified, but more importantly, it requires that the spectrum of references is largely unchanged in each sample. Small changes in structure, or crystallinity if the materials is a solid, can affect the EXAFS spectrum, and make it hard to apply. This fitting method is based on interatomic distances that are fit based on theory alone, and thus are independent of reference selection. That said, this method is relatively insensitive to minor components that lack well defined structural features to identify them. The conversion of coordination numbers to a species abundance implies a direct conversion, however it is conceivable that additional species are present that are combined with more abundant species with similar interatomic distances. For this reason, we refer to Zn-NA complexes as a combination of Zn-NA complexes and mineral forms of Zn, most of which have Zn in octahedral coordination with oxygen.

Results & discussion

Soil Zn concentration and deficiency

The soils used for rice cultivation in this work have widely variable chemical compositions and textures (Table 2). Based on the total amount of Zn, we divided the samples into two groups, the group less than the Zn detection limit and the group above the Zn detection limit. The difference between these two groups of samples reflects, to some extent, the



 Table 2
 Soil properties and Zn deficiency for cambodian paddy soils

Sample ID	Sampling date	Hd	Soil texture	Eleme in soil	Element concentration in soil (mg kg ⁻¹)	tration)	DTPA extractable (mg kg ^{-1–})		Main soil Zn deficiency factors	SS		Soil bioavail- able Zn level ^e	Soil Zn deficiency level ^f
				Zu	Fe	S	Zn	Total Zn ^a	Soil Texture ^b	Total Fe °	Total S ^d		
KCH119_102R	Nov. 2018	<i>L</i> -9	Clay	111	6445	833	0.35		+		1	Higher	Lower
KCH119_104R	Nov. 2018	2-9	Clay	10	11,116	669	0.34		+	1	,	Higher	Lower
KPC119_8R	Nov. 2018	6-7	Clay	10	6100	778	0.29		+	1	,	Higher	Lower
PP119_22R	Nov. 2018	2-9	Sand	^ 4	4468	644	0.12	++	ı			Lower	Higher
PP119_2R	Nov. 2018	2-9	Sand	6	2613	912	0.21		ı	+	,	Higher	Lower
PP119_3R	Nov. 2018	2-9	Silt	6	2613	912	0.1		ı	+	,	Higher	Lower
PP119_103R	Nov. 2018	2-9	Sand	^	878	966	<0.1	++	ı	++	1	Lower	Higher
PP119_13R	Nov. 2018	2-9	Sand	4>	829	932	< 0.1	+++	ı	++	1	Lower	Higher
PP3_Rice1	Jan. 2019	2-9	Sand	4>	2400	816	< 0.1	+++	ı	+	ı	Lower	Higher
PP3_Rice2	Jan. 2019	6-7	Sand	4	2400	816	<0.1	+++	ı	+	1	Lower	Higher
PP5_Rice1	Jan. 2019	6-7	Sand	4	2400	816	< 0.1	+++	ı	+	1	Lower	Higher
PP6_Rice1	Jan. 2019	6-7	Sand	4	2400	816	< 0.1	+++	ı	+	1	Lower	Higher
PP7_Rice1	Jan. 2019	2-9	Sand	4	1400	848	< 0.1	+++	ı	++	ı	Lower	Higher
PT3_Rice1	Jan. 2019	6-7	Clay	70	34,500	845	0.31		+	1	1	Higher	Lower
PT5_Rice1	Jan. 2019	6-7	Clay	4	2800	850	0.29	++	+	+	1	Lower	Higher
PT8_Rice1	Jan. 2019	2-9	Clay	4	2800	850	0.34	++	+	+	ı	Lower	Higher

(a): Primary deficiency factor, Zn deficiency is presumed when soil Zn is low (<4 mg kg⁻¹ (limit of detection, LOD)), while Zn is considered replete (sufficient) when soil Zn is

^b: Zn deficiency related to soil texture; all the sandy soil are considered less at risk of Zn deficiency than clay soils if Zn concentrations are similar;

(°): Zn deficiency is associated with low (<2000 mgFe kg⁻¹) levels of Fe in paddy soil, concentrations of 2000-3000 mg kg⁻¹ are considered potentially ow enough to induce defi-

(^d): S levels are all near levels sufficient to induce sulfide precipitation

(°): Identification of soil bioavailable Zn based on the combination of soil composition and texture;

(f): Identification of rice growing Zn deficiency possibility based on the combination of soil composition and texture;

(++): Indicative of more extensive Zn deficiency (relative to typical rice-growing soils);

(+): Indicative of potential Zn deficiency;

(-): Indictive to no Zn deficiency or minimal deficiency;

XRF analysis quality control was shown in Table S1 in supporting information



difference in the severity of Zn deficiency in the soils we collected. Most relevant to this study are total and extractable Zn levels in each soil. Zinc deficiency in soil is a common problem in Cambodia (Blair and Blair 2014) for one of four major reasons:

- 1. Low total and extractable Zn concentrations. The bioavailability of Zn is commonly assessed by measuring the concentration of Zn extracted from soil using DTPA, or somewhat less precisely, based on total Zn concentrations. Normally, DTPA-extractable Zn in soils < 0.8 mg kg⁻¹ is associated with Zn deficiency in rice (Dobermann and Fairhurst 2000). DTPA extractions of the soils in this study are all uniformly low, ranging from $< 0.1 \text{ mg kg}^{-1}$ to about 0.3–0.4 mg kg⁻¹. Using this definition, Zn nutrient status varies widely but all the soils in this study are Zn deficient. Care must be used in evaluating DTPA extractions, however, as measurements performed in dry soils are often not representative for flooded soils because Zn availability can vary temporally (Johnson-Beebout et al. 2009). As such, we define Zn deficiency based on total Zn levels in the soil. DTPA-extractable Zn typically is only 1-2% of the total Zn in tropical paddy soils in South Asia (Wisawapipat et al. 2017). This implies that soils are likely to be Zn deficient if they contain < 25-50 mg kg⁻¹ Zn. Accordingly, we conservatively define paddy soils as highly deficient if they have total Zn concentrations less than the limit of detection (LOD, about 4 mg kg⁻¹) and potentially somewhat inadequate at levels up to 25 mg kg⁻¹. This designation is also supported by the fact that Zn levels in rice plants are correlated to soil Zn in this concentration range (Rutkowska et al. 2013).
- 2. Flooding-Induced Zn Mineral Precipitation. Flooding affects Zn availability by changing the chemical form of Zn. Flooding induces sulfate reduction to sulfide followed by the precipitation of insoluble sulfides, decreasing bioavailability (Du Laing et al. 2007). The amount of flooding varied considerably between sites during sampling and between growing seasons in this study, potentially modulating Zn deficiency, but this effect could not be tracked in this research, and it is not used to distinguish between different rice samples. Normally, sulfide mineral precipitation

- requires adequate sulfate to be present. For flooding conditions, S concentrations > 100 mg kg⁻¹ is sufficient to form ZnS (Bunquin et al. 2017). In these soils, all soils have sufficient S (600–1000 mg S kg⁻¹) to allow for ZnS precipitation during flooding.
- 3. Low Soil Fe Concentrations. Soil Fe oxides often are effective at buffering sulfide concentrations to levels too low for ZnS precipitation and thereby maintaining Zn solubility and bioavailability when soils are flooded (Bunquin et al. 2017). Iron oxides also adsorb Zn but release that Zn into solution during reductive dissolution (Du Laing et al. 2009). Zn deficiency thus is often associated with low total soil Fe (<1500 mg kg⁻¹). Here total Fe above 4000 mg kg⁻¹ was considered as low Zn deficiency possibility, while 1500–4000 mg kg⁻¹ was considered as some possible Zn deficiency risk, and less than 1500 mg kg⁻¹ was considered as definitely high Zn deficiency risk.
- 4. Other Factors. Soil texture correlates to total Zn concentrations, and also affects Zn bioavailability and the retention of soluble Zn because the sandy paddy soils are essentially quartzose sands and have very low (a few ppm) total Zn. Soil texture also affects water dynamics and microbial community, almost certainly influencing how the redox cycling occurs. Given that the sandy soils are also low in Fe, it is likely that those sandy soils also have less buffering of sulfide in porewaters, potentially enhancing ZnS precipitation. Zn fertilizer is more available in sandy soils than clayey soils (Rutkowska et al. 2013), but soluble Zn also is easily leached from sandy soil. Here in our study, no Zn fertilizer is applied to any soils and all the sandy soils are extensively leached with Zn concentrations lower than clay soils and well below limiting thresholds. As such, most sandy soils are likely Zn-limited. Other factors also could play secondary roles. For example, soil pH affects metal solubility by influencing the formation of metal complexes with dissolved organic carbon (DOC), precipitation of carbonate phases, and the adsorption of Zn to Fe and Mn (hydro)oxides (Kirk 2004). DOC also has a limited effect in this study because all the soils are pH 6–7. However, for other studies (pH > 7), this part may be important and cannot be ignored.



Based on these factors, these two groups divided with total amount of Zn were relative to low-Zn and likely Zn-deficient, or moderate to high-Zn and indicative of moderate Zn availability and less Zn-limited (Table 2). This classification is conservative in that it probably underestimates Zn deficiency, and it does not account for the potential effects of rice variety (Alloway 2009; Wissuwa et al. 2008). Independent sample t-test was used for analysis analyses of statistical differences.

Rice chemical composition

Although total Zn concentrations in paddy soils varied by nearly 2 orders of magnitude, the Zn level of rice grown was consistently 15–30 mg kg⁻¹ and was not correlated to soil total Zn levels (Table 3). Pooled analysis that grouped rice samples based on their Zn fertility status, however, does reveal a small and statistically insignificant difference in grain chemical composition (Fig. 1). Rice grown in soils with lower

soil Zn levels have variable but somewhat higher grain Zn concentrations than rice samples grown in soils with higher Zn levels, and similar to market rice samples. Most rice samples in both groups clustered between the interquartile range of 18–25 mg kg⁻¹ Zn. This likely reflects the homeostasis in Zn concentrations in rice grains. Rather than producing rice grains that have too little Zn to be viable, the rice plant either grows less or produces fewer grains under limiting conditions. Unfortunately, yield information from each site is not well documented in this study. These Zn concentrations that are observed are consistent with Zn concentrations typical of rice grown under Zn deficient (<25 mg kg⁻¹) or borderline sufficient (18–35 mg kg⁻¹) soil conditions (Wissuwa et al. 2008), and our conservative estimates of Zn deficiency based on soil composition (Table 2).

Genotype or rice variety also can affect nutrient uptake, nutrient storage, and overall susceptibility to nutrient limitation (Alloway 2009; Wissuwa et al.

Table 3 Concentrations of Zn and selected elements in Cambodian rice grain

Sample ID	Sampling date	Rice variety	Element concentration (mg kg ⁻¹)						
			Zn	P	S	Fe	Cu	Mn	
KCH119_102R ^(a)	Nov. 2018	Rice 85	15.7	3417	1304	7.46	0.98	16.3	
KCH119_104R ^(a)	Nov. 2018	Rice 85	17.7	852	1105	0.86	2.49	10.2	
KPC119_8R ^(a)	Nov. 2018	Tgon, Rice 85, Pka Mleas	20.1	2415	1023	4.65	2.36	28.3	
PP119_22R(b)	Nov. 2018	Unknown	24.2	2868	872	3.29	1.37	16.0	
PP119_2R ^(a)	Nov. 2018	Chhmar Prom	19.9	1851	985	4.70	1.63	19.1	
PP119_3R ^(a)	Nov. 2018	Chhmar Prom	22.1	2866	1051	7.70	2.06	23.4	
PP119_103R(b)	Nov. 2018	Srov Khmao	18.1	2391	880	3.07	1.83	21.8	
PP119_13R(b)	Nov. 2018	Chhmar Laet	20.8	2371	1159	4.07	3.27	43.1	
PP3_Rice1 ^(b)	Jan. 2019	Romdol	27.3	3773	902	14.10	2.48	20.7	
PP3_Rice2 ^(b)	Jan. 2019	Romdol	26.1	3724	876	9.00	1.80	20.3	
PP5_Rice1 ^(b)	Jan. 2019	Romdol	24.9	3610	869	10.96	1.00	27.2	
PP6_Rice1 ^(b)	Jan. 2019	Unknown	29.7	3593	900	15.06	1.85	21.4	
PP7_Rice1 ^(b)	Jan. 2019	Chonarlar	23.6	3119	985	11.25	3.88	42.0	
PT3_Rice1 ^(a)	Jan. 2019	Unknown	15.3	2479	756	9.78	2.73	24.4	
PT5_Rice1 ^(b)	Jan. 2019	Unknown	27.8	3352	1047	11.33	2.76	29.3	
PT8_Rice1 ^(b)	Jan. 2019	Unknown	16.4	2876	883	10.57	2.76	24.8	
Market2 ^(c)	-	China (black rice)	13.4	2449	891	5.25	1.43	26.5	
Market3(c)	-	Thai (sweet rice)	18.3	511	939	2.09	1.50	7.4	
Market9 ^(c)	-	Thai (Red cargo rice)	19.7	2471	916	3.52	1.96	23.6	

⁽a): Rice grains are grown in soil with less Zn deficiency (high soil bioavailable Zn);

^{(-):} Not available



⁽b): Rice grains are grown in soil with more Zn deficiency (low soil bioavailable Zn);

⁽c): Market rice grains are grown under unknown levels of Zn deficiency;

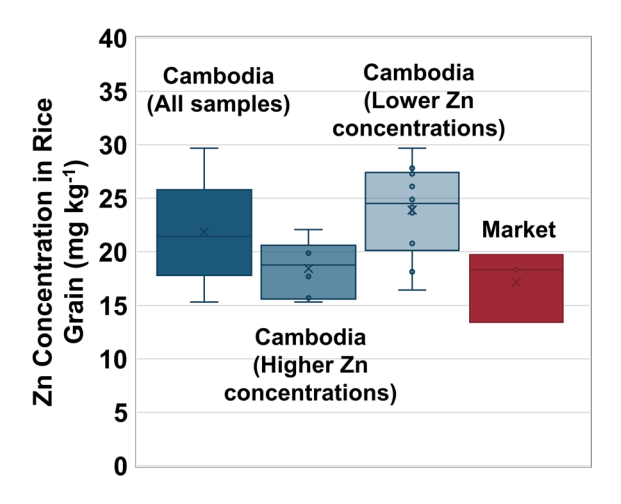


Fig. 1 Zn concentrations in rice grains collected from paddy soils in Cambodia compared with market rice samples from China and Thailand. Cambodia (All samples): All rice grain samples collected from Cambodia with variable Zn deficiency degrees (n=16). Group Cambodia (All samples) is divided into two groups based on total and bioavailable Zn concentrations. Cambodia (Higher Zn concentrations) identified as grown in soil with higher soil Zn concentrations (low Zn deficiency, n=6). Cambodia (Low Zn concentrations) identified as grown in soil with low soil Zn levels (moderate and higher levels of Zn deficiency, n=10). Market is rice samples (Zn deficiency condition unknown) (n=3). The box and whisker plot shows the minimum value, first quartile, median, third quartile and maximum value of the data group. An independent sample t-test was used for analysis analyses of statistical differences. Significant difference (p < 0.05) between Cambodia (Low Zn concentrations) and Cambodia (Higher Zn concentrations) was found. Significant difference (p < 0.05) between Cambodia (Lower Zn concentrations) and Market was found. Most of Cambodia rice samples have 15-30 mg kg⁻¹ Zn regardless of Zn deficiency, reflecting physiological changes to maintain Zn homeostasis in the grain

2008). Despite this fact, this study does not control for rice variety. In fact, within our sampled sites, nearly half of all rice samples were a unique variety, and only a few varieties were sampled more than a few times. In contrast, more developed agricultural systems like the US or China typically grow only a few varieties of rice. The genetic diversity of commonly-cultivated Cambodian rice is much higher; there are over 2500 rice varieties grown in Cambodia, most isolated to a few growing areas or growth conditions (Sar et al. 2012). These Cambodian rice varieties are not well characterized but chosen based on local experience, in many cases probably favoring the ability to grow under more variable nutrient

availability and water stress conditions common to under-fertilized crops and irregular rainfed irrigation. In most cases, the net result of growing these unimproved/native varieties of rainfed rice adapted to growth with minimal fertilizer inputs only has a single crop per year with lower overall yields, often < 3 tons ha⁻¹ (Blair and Blair 2014).

Zn localization in rice embryo, aleurone, and endosperm

Zinc in grains facilitates protein synthesis, cell elongation, membrane function, and resistance to abiotic stresses during germination (Cakmak 2000; Farooq et al. 2012). The embryo is the nascent growing plant, and it is often enriched in metals including Zn because protein synthesis and cellular functions are localized there. The aleurone layer is a proteinaceous layer on the outer part of the endosperm that is responsible for nutrient uptake during grain filling. The embryo and aleurone layer typically have concentrations of metals higher than the endosperm (Bewley et al. 2013), and thus are assumed to be the important sources of nutrients to emergent seedlings. However, the endosperm may also be an important nutrient source because it is larger, and thus could contain a significant fraction of total metals even if they are found in low concentrations.

XRF-measured elemental distributions indicate that most elements are heterogeneously distributed within the rice grain (sample KPC-119–3, Fig. 2). Zn levels are much higher in the embryo and aleurone than in the endosperm, which is similar to previous reports (Takahashi et al. 2009), and Fe, Zn, S, Mn, and P have similar distributions. Within the embryo, Zn concentrations are also somewhat heterogeneously distributed, with higher Zn levels associated with the radicle than the plumule. Nutritional elements like Ti, originating primarily from inorganic sources such as soil, exhibit minimal concentrations (near the detection limit) but are found concentrated on grain surfaces. Importantly, the aleurone is preserved in our analysis, indicating that the method used to remove the husk was sufficient to remove the rice husk without also removing the aleurone and embryo.

The total quantity of each element within the embryo, aleurone, and endosperm (the major divisions of the grain) is estimated by sectioning the



Fig. 2 Element localization in rice grain cross-section sample (KPC_119-3) collected from Cambodia based on µ-XRF. Most elements are heterogeneously distributed in rice grain. Zn, Fe, P, Cu, S, Mn, and Ti levels are much higher in the embryo and aleurone than in the endosperm (shown in the grain section map), suggesting Zn is highly possible combined with P and S in embryo and aleurone layer. Most elements are biologically cycled. $Log(I_0/I_1)$, sample absorption, is a function of sample thickness, showing that the rice is thickest in the center

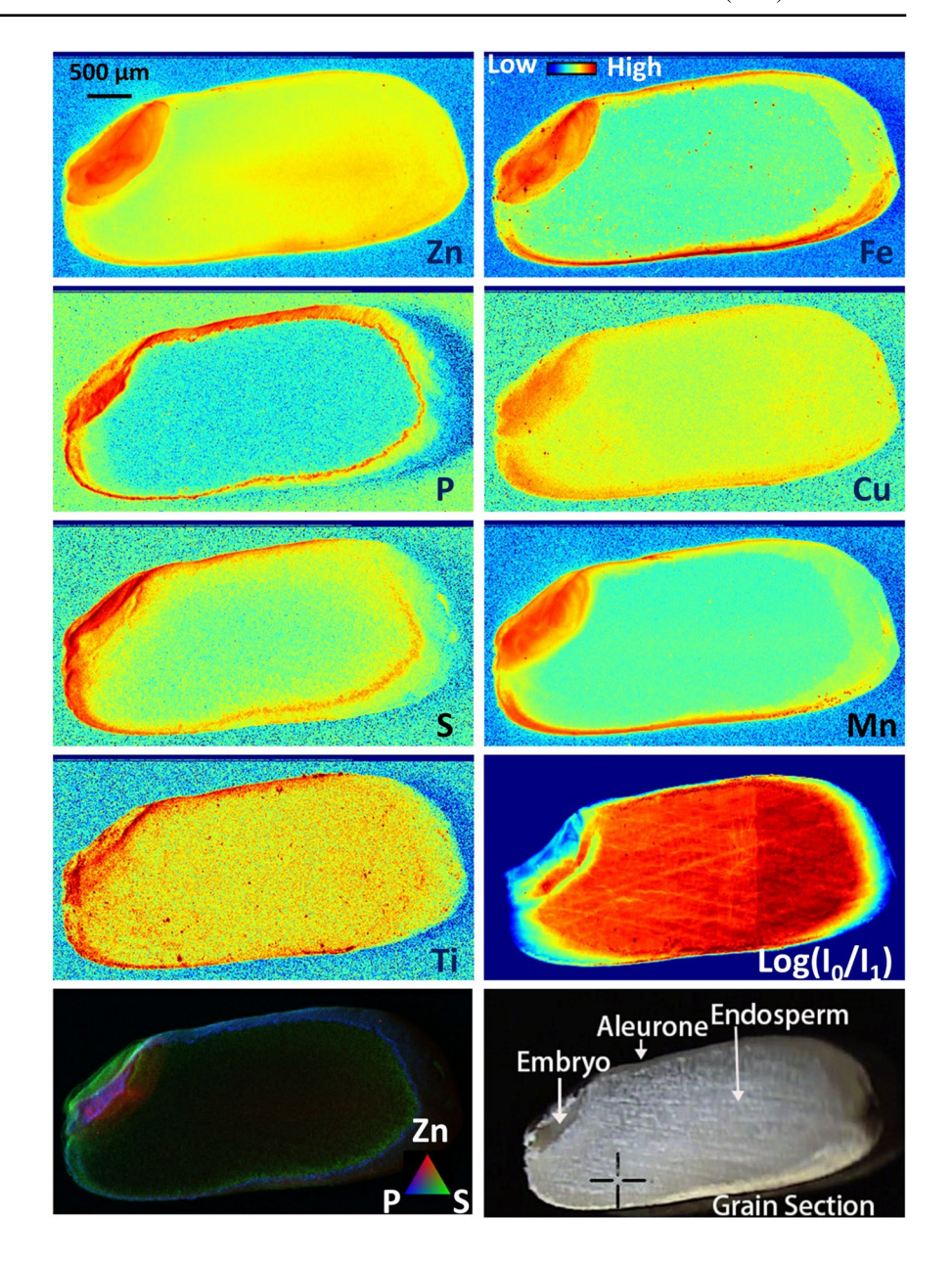


image into their corresponding areas or regions using masking tools (Fig. S2). Using these, we can calculate the mean and variance of each element concentration relative to the endosperm within each masked area (Fig. 3a). By summing the counts or relative element concentrations within each region (Webb 2011), we can estimate the percentage of a given element in different tissues corresponding to these masks (Fig. 3b). This analysis indicates that most elements are most concentrated in the embryo, including Zn, but more abundant overall in the endosperm because

of its higher volume. Iron and Si are notable exceptions that are more concentrated in the aleurone, but also are largely in the endosperm. For Fe, this could reflect the accumulation of Fe in storage compounds within the aleurone (Fig. 2).

The concentration ratios for Zn in embryo, aleurone and endosperm are 5.7: 1.3: 1. For comparison, Zn concentrations of embryo and endosperm in barley are 164 mg kg⁻¹ and 14 mg kg⁻¹ (Persson et al. 2009), corresponding to a ratio of 11.7 (Table S2). Although the embryo contains > 5 times higher Zn



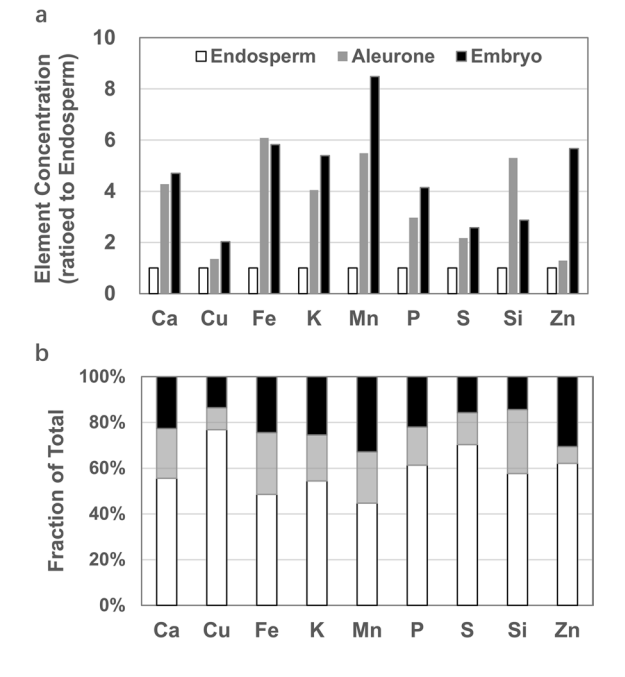


Fig. 3 (a) Average element concentration in the embryo, aleurone and endosperm (unitless, normalized to the endosperm), and (b) the calculated distribution (in percent) of each element between the embryo, aleurone and endosperm. The endosperm has the lowest average concentrations of most elements, relative to the aleurone and embryo, including Zn, P, S, and Cu. However, more than 60% of those elements are stored in endosperm

concentrations than that in the endosperm, it contains around 30% of the total Zn because it is small relative to the endosperm and aleurone. The aleurone and endosperm have similar Zn concentrations, but the endosperm contains 60% of the total Zn because of its large size (Fig. 3b). This differs from other studies that suggest Zn is localized primarily in the aleurone as phytate complexes stored in protein storage vacuoles (Raboy 2009; Bohn et al. 2008). In this case, it is likely that this difference stems from the fact that this study directly measures the locations of Zn and P localization, while most other work either infers it based on biological function, or operationally defines differences using ex situ approaches like extractions.

Element concentration maps of P and S are particularly relevant in this study because phosphorus and sulfur (as thiol) potentially complex Zn. Most P in grains is usually present as phytate, while much of S is associated with proteins. The distribution of P (and thereby phytate) is similar to that of Zn, while S is more evenly distributed (Fig. 2). In this study, the

relative concentration ratios of P and S in embryo, aleurone and endosperm are around 4.1:3.0:1 and 2.6: 2.1:1, respectively (Fig. 3a). Our results, however, suggest that much more P and S are stored in the endosperm (80% for P) than in the aleurone. Our higher estimates of endosperm-associated-Zn and P than previous estimates (Raboy 2009; Bohn et al. 2008) may reflect differences in analysis methods, rice variety or growth conditions.

The spatial correlations of Zn:P and Zn:S count ratios also can be used to better understand how Zn in retained in these phases. The relationship between Zn and S or P depends on which region of the grain is analyzed, suggesting it might be bound in different environments in each (See supporting information part 2, Figs. S3 and S4). Zn counts correlate with P counts within the embryo, suggesting that Zn may be associated with P, or enriched in parallel to P, in that tissue. There is a much weaker or absent correlation between Zn and P in endosperm and aleurone, suggesting that only a small portion of the P is also associated with Zn in these regions (Fig. S3). Similar features have been found by previous authors (Liang et al. 2008). In contrast, wheat was characterized differently from rice, and a better correlation between Zn and P was found in aleurone (Persson et al. 2016), which shows that there may be differences in Zn species and their location in different small grain cereals. The slope of the Zn:P ratio also provides potential information about the relative importance of P to Zn complexation in specific tissues. The magnitude of the Zn:P ratios/slopes follow the order of aleurone < embryo < endosperm. Given that the aleurone has much higher P levels (and presumably also higher phytate concentrations) than other regions (Raboy 2009; Bohn et al. 2008; Iwai et al. 2012), the low Zn:P ratio suggests that Zn only complexes a small fraction of the total P/phytate in the aleurone, and that much of the aleurone's phytate is stored in vacuoles with other metals. In contrast, the endosperm contains less P and phytate, but Zn is a more significant portion of metals bound in those regions. Minimal correlations between Zn and S are found in any of these three tissues (Fig. S4). This correlation might be observable if much of the Zn was bound to protein, which commonly binds Zn through thiol groups in cysteine. Thus, it appears that protein or other thiol-bound Zn is an insufficient portion of total Zn or S levels to produce a correlation, and



minor relative to its complexation in more abundant storage compounds.

Zinc local structure and speciation in rice grain

Bulk (whole-grain) EXAFS spectra of each rice sample contained a combination of tetrahedral Zn–O, octahedral Zn–O and tetrahedral Zn–S indicative of the primary Zn species present: Zn-Phytate, Zn-NA (or mineral Zn containing octahedral Zn–O) and Zn-protein/thiol (Table 4, example fits are shown in Fig. S5). Also present in each sample is a distinct Zn-P shell at 3.1 Å consistent with Zn in phytate. In

most cases, tetrahedral Zn–O coordination predominates and is accompanied by the presence of two Zn-P second-shells, indicating that Zn-phytate is the most abundant form of Zn in the grain.

The relative fraction of each Zn species has been quantified in 19 rice samples (Table 5) based on their coordination environments (Table 4). Zn-phytate was most abundant, with 66–88% of Zn identified as combined with phytate Zn, and around 10–29% of Zn is combined with NA or as Zn minerals. The proportion of Zn combined with protein or other thiols is very limited (2%-11%) and insignificant (with estimated errors over the fractional abundance). Consequently,

Table 4 Structural parameters determined by simulating extended X-ray absorption fine structure (EXAFS) spectra for Zn in rice grain

Sample ID	Coordination	number ± uncerta	inty			χ2	Reduced χ2	R factor
	Zn-O tet [Zn Phytate] (1.95 Å)	Zn–O oct [Zn-NA/min- eral] (2.11 Å)	Zn-S tet [Zn Thiol/Protein] (2.34 Å)	Zn-P ^(*) [Zn Phytate] (3.1 Å)	Zn-P ^(*) [Zn Phytate] (3.6 Å)			
KCH119_102R ^(a)	3.0 ± 0.6	0.7 ± 0.8	0.4 ± 0.5	1.0 ± 0.7	3.9 ± 1.0	150.26	23.25	0.0175
KCH119_104R ^(a)	2.9 ± 0.7	1.0 ± 0.9	0.5 ± 0.5	2.0 ± 0.6	4.9 ± 1.0	62.37	9.65	0.0165
KPC119_8R ^(a)	2.5 ± 0.4	1.0 ± 0.5	0.2 ± 0.3	1.1 ± 0.4	3.0 ± 0.6	96.28	14.89	0.0088
PP119_22R(b)	2.6 ± 0.4	0.9 ± 0.5	0.1 ± 0.3	1.1 ± 0.4	2.9 ± 0.6	79.09	12.23	0.0102
PP119_2R ^(a)	2.9 ± 0.5	1.3 ± 0.5	0.2 ± 0.4	1.1 ± 0.6	3.2 ± 1.0	58.55	9.06	0.0171
PP119_3R ^(a)	2.5 ± 0.4	1.0 ± 0.5	0.3 ± 0.3	1.1 ± 0.4	2.9 ± 0.6	154.16	23.85	0.0077
PP119_103R(b)	3.4 ± 0.5	0.6 ± 0.7	0.2 ± 0.4	2.1 ± 0.4	4.1 ± 0.7	19.48	3.01	0.0076
PP119_13R ^(b)	3.3 ± 0.5	0.8 ± 0.6	0.4 ± 0.4	1.0 ± 0.7	2.8 ± 1.0	41.57	6.43	0.0152
PP3_Rice1 ^(b)	3.3 ± 0.5	0.6 ± 0.7	0.3 ± 0.4	1.4 ± 0.6	3.7 ± 0.9	58.65	9.07	0.0121
PP3_Rice2 ^(b)	3.1 ± 0.5	1.0 ± 0.6	0.3 ± 0.4	1.1 ± 0.5	3.2 ± 0.8	32.96	5.10	0.0104
PP5_Rice1 ^(b)	3.1 ± 0.5	1.1 ± 0.5	0.3 ± 0.4	1.1 ± 0.5	3.2 ± 0.8	315.01	48.74	0.0098
PP6_Rice1(b)	3.2 ± 0.5	0.8 ± 0.6	0.2 ± 0.4	1.2 ± 0.7	3.3 ± 1.1	82.70	12.79	0.0197
PP7_Rice1 ^(b)	3.4 ± 0.5	0.5 ± 0.6	0.1 ± 0.4	1.2 ± 0.5	3.6 ± 0.8	28.37	4.39	0.0097
PT3_Rice1 ^(a)	2.9 ± 0.7	1.1 ± 0.8	0.3 ± 0.5	1.8 ± 0.4	4.5 ± 0.6	22.45	3.47	0.0072
PT5_Rice1 ^(b)	3.4 ± 0.5	0.6 ± 0.7	0.2 ± 0.4	1.5 ± 0.5	3.9 ± 0.8	44.19	6.83	0.0096
PT8_Rice1 ^(b)	3.5 ± 0.5	0.4 ± 0.7	0.1 ± 0.4	1.2 ± 0.6	3.4 ± 0.9	53.76	8.32	0.0127
Market2 ^(c)	3.0 ± 0.6	1.0 ± 0.8	0.5 ± 0.4	1.5 ± 0.6	3.8 ± 0.9	36.31	5.62	0.0135
Market3 ^(c)	3.0 ± 0.7	0.8 ± 0.9	0.5 ± 0.5	2.2 ± 0.6	4.9 ± 1.0	75.21	11.63	0.0155
Market9 ^(c)	3.1 ± 0.5	1.0 ± 0.6	0.2 ± 0.4	1.3 ± 0.5	3.4 ± 0.8	31.11	4.81	0.0102

The tetrahedral Zn–O likely represents Zn phytate complexes, the octahedral Zn–O is likely representative of Zn nicotianamine (NA) complexes or Zn mineral, and a tetrahedral Zn–S represents Zn thiol complexes similar to those found for Zn bound to thiols in proteins

⁽c): Market rice grains are grown under unknown levels of Zn deficiency



^{(*):} The structural parameters from the Zn-P shell are determined in independent fits with fixed Zn-O/S coordination numbers to reduce the number of fit variables;

⁽a): Rice grains are grown in soil with less Zn deficiency (high soil bioavailable Zn);

⁽b): Rice grains are grown in soil with more Zn deficiency (low soil bioavailable Zn);

Plant Soil (2023) 491:605-626

Table 5 The normalized component fractions of different Zn components present in rice grain based on coordination numbers obtained by extended X-ray absorption fine structure (EXAFS) shell fitting and presented in Table 4

Sample ID	Normalized compo	nent fraction ± uncertainty		Normaliza-	
	Zn–O tet [Zn Phytate] (1.95 Å)	Zn–O oct [Zn-NA/mineral] (2.11 Å)	Zn–S tet [Zn Thiol/Protein] (2.34 Å)	tion factor	
KCH119_102R ^(a)	0.77 ± 0.16	0.12±0.14	0.11 ± 0.12	0.96	
KCH119_104R ^(a)	0.72 ± 0.17	0.17 ± 0.15	0.12 ± 0.13	1.02	
KPC119_8R ^(a)	0.75 ± 0.13	0.20 ± 0.09	0.05 ± 0.10	0.83	
PP119_22R(b)	0.85 ± 0.14	0.09 ± 0.12	0.05 ± 0.11	1.01	
PP119_2R ^(a)	0.79 ± 0.11	0.12 ± 0.10	0.09 ± 0.09	1.04	
PP119_3R ^(a)	0.78 ± 0.12	0.18 ± 0.09	0.04 ± 0.09	0.82	
PP119_103R(b)	0.75 ± 0.13	0.21 ± 0.09	0.04 ± 0.10	0.98	
PP119_13R ^(b)	0.73 ± 0.12	0.19 ± 0.09	0.08 ± 0.09	0.84	
PP3_Rice1 ^(b)	0.82 ± 0.13	0.10 ± 0.12	0.08 ± 0.10	1.01	
PP3_Rice2 ^(b)	0.76 ± 0.12	0.16 ± 0.09	0.08 ± 0.09	1.01	
PP5_Rice1 ^(b)	0.75 ± 0.12	0.19 ± 0.09	0.07 ± 0.09	1.03	
PP6_Rice1 ^(b)	0.81 ± 0.13	0.14 ± 0.11	0.05 ± 0.10	0.99	
PP7_Rice1 ^(b)	0.89 ± 0.13	0.09 ± 0.11	0.02 ± 0.10	0.97	
PT3_Rice1 ^(a)	0.73 ± 0.17	0.19 ± 0.13	0.08 ± 0.13	0.99	
PT5_Rice1 ^(b)	0.86 ± 0.14	0.10 ± 0.12	0.04 ± 0.11	1.00	
PT8_Rice1(b)	0.90 ± 0.13	0.07 ± 0.11	0.03 ± 0.10	0.97	
Market2 ^(c)	0.73 ± 0.14	0.16 ± 0.12	0.11 ± 0.11	1.03	
Market3 ^(c)	0.75 ± 0.17	0.13 ± 0.15	0.11 ± 0.13	1.00	
Market9 ^(c)	0.79 ± 0.13	0.16 ± 0.10	0.05 ± 0.10	1.00	

The tetrahedral Zn–O likely represents Zn phytate complexes, an octahedral ZnO is likely representative of Zn nicotianamine (NA) complexes or Zn mineral, and a tetrahedral ZnS represents Zn binding with thiol complexes similar to those found for Zn bound to thiols in proteins. The normalization factor accounts for the fit coordination numbers of ZnO tet, ZnO oct and ZnS tet using defined Debye–Waller factors as described in the experimental section). Reported uncertainties reflect variable uncertainty, correlation, fit and data quality

- (a): Rice grains are grown in soil with less Zn deficiency (high soil bioavailable Zn);
- (b): Rice grains are grown in soil with more Zn deficiency (low soil bioavailable Zn);
- (c): Market rice grains are grown under unknown levels of Zn deficiency

we also report quantitative results omitting the Zn–S shell entirely, which increases the relative proportion of the other Zn phases slightly (Table S3). Thus, EXAFS indicates that most Zn is bound principally in phytate complexes, which are mostly not bioavailable, with smaller fractions of more available organic complexes or mineral phases.

EXAFS results indicate that Zn-phytate is abundant in rice grains. Our XRF results help constrain where this Zn-phytate is localized in the grain. The μ -XRF results indicate that more than 60% of Zn in rice grain is stored in the endosperm, similar to the fractions of Zn-phytates calculated by EXAFS fitting. This combination of findings could result if all of

the Zn bound in phytate is present in the endosperm; however, μ-XRF results (Fig. 2) also indicate that much of the rice P (and thus most phytate) is localized in the aleurone. We thus conclude that Zn phytate is distributed in all tissues. For example, if all of the Zn in aleurone and embryo is assumed to be associated with phytate, at least (15–35%) of Zn would still need to be present as Zn-phytate complexes within the endosperm to explain its overall prevalence in the grain. There is limited information to confirm these associations in rice, but it appears that Zn is complexed with phytate in the endosperm and other portions of the grain (Iwai et al. 2012). Zn-NA or mineral Zn also seems to be somewhat



more abundant and correlated to Zn concentrations in embryos (r=0.647, significant at P<0.05) (Díaz-Benito et al. 2018). If the Zn is bound within mineral forms, this could reflect the precipitation of mineral grains potentially as storage compounds within this layer, similar to phytate complexes stored there. Alternatively, Zn-NA/mineral may be stored in the aleurone or embryo. Given these constraints, we conclude that the Zn-phytate and NA/mineral complexes are found in all tissues, but that Zn-NA/mineral complexes are somewhat more abundant in aleurone and embryo, while Zn-phytate is slightly more abundant in the endosperm.

Linking soil Zn deficiency to rice Zn speciation and bioaccessibility

The chemical form of Zn in the studied rice samples is related to the total Zn concentration in those grains (Fig. S6). In general, phytate Zn and mineral Zn content are somewhat correlated with total Zn in the grain (in mg kg⁻¹ of each species, calculated with the fraction of each species and the XRF-measured Zn concentration in the grain). This correlation across all samples implies that there is a systematic relationship between total Zn and the speciation of that Zn.

Because this study examines both the rice and the soil from which the rice was grown, it is possible to qualitatively attribute variation in growing conditions and Zn availability to the structure of Zn bound in rice, and thus to the chemical form and concentration of Zn in rice. There is a significant (P < 0.05) increase in the coordination number of tetrahedral Zn-O (2.7 to 3.2) that accompanies a decrease in the coordination number of octahedral Zn-O (1.0 to 0.7) in more Zn-limited rice samples, while coordination of Zn to S is low (<0.4) but not affected (Fig. 4 (a, b and c)). This change in coordination indicates that Znphytate becomes more abundant under Zn deficiency, while Zn bound to nicotianamine or other octahedral forms decreases. The P:Zn ratios in the soils of all samples were regressed on tetrahedral Zn-O, octahedral Zn-O and tetrahedral Zn-S coordination and a good linear positive correlation was found between P:Zn and tetrahedral Zn-O coordination (Pearson correlation coefficient = 0.641, p < 0.01) (Fig. 4 (d)). It was reported that Zn co-fertilized with appropriate P is an effective strategy to enhance P availability in rice rhizosphere soil to improve plant growth and P uptake (Lv et al. n.d.). This may imply that under Zn-deficient conditions, a soil P/Zn bioavailability change or disproportionality in the soil may be some key factor affecting Zn species, especially phytate-Zn in the rice grain.

The level of Zn deficiency significantly (P<0.05) affects concentrations of Zn phytate and Zn-NA/mineral (Fig. 5). Zn-phytate concentrations increase about 10% (almost 5 mg kg⁻¹ in concentration) under higher levels of deficiency. This increase in phytate is matched by a corresponding 7% (~3 mg kg⁻¹) decrease in the concentration of Zn-NA/mineral, and to some extent by a statistically significant increase in the total concentration of Zn. In contrast, Zn bound to thiols in proteins are small but unaffected by nutrient status.

Paradoxically, total Zn levels in grain appear to increase slightly in response to lower Zn fertility, in parallel with increases in fractional Zn-phytate concentrations (Fig. 5). We can further study this relationship by examining how grain Zn and P concentrations vary as a function of Zn concentration in soil (Fig. 6). In Zn-deficient soils, grain Zn concentrations in grain are generally higher than in soils where Zn is more abundant. In Zn-deficient soils, grain Zn concentrations also increase with grain P content (which is primarily present in phytate), in contrast to soils where Zn is more abundant. This is unexpected given that lower Zn levels in soils would presumably decrease its bioavailability and uptake. This apparent inconsistency, however, is explained by changes in yield and physiological response to nutrient deficiencies. The most pronounced effect of nutrient deficiency is diminished growth and lower crop yields. Thus, the nutrient deficiency that decreases the amount of grain produced can lead to overall less Zn uptake, even if the concentration of Zn in that grain stays constant or potentially increases. The physiological response to Zn deficiency is the induction of Zn uptake, the increased production of phytate in the grain, leading to an increase in phytate that can increase Zn concentrations. Overall, this increased Zn uptake is modest and the benefits it brings do not counter the effect of yield loss due to nutrient deficiency. Our data suggest that homeostasis effectively regulates Zn levels in the grain to ensure that grain produced is viable. Future studies should measure grain yields, and control for rice variety differences, consider synergistic effects between Zn and other nutrients (Khampuang et al.



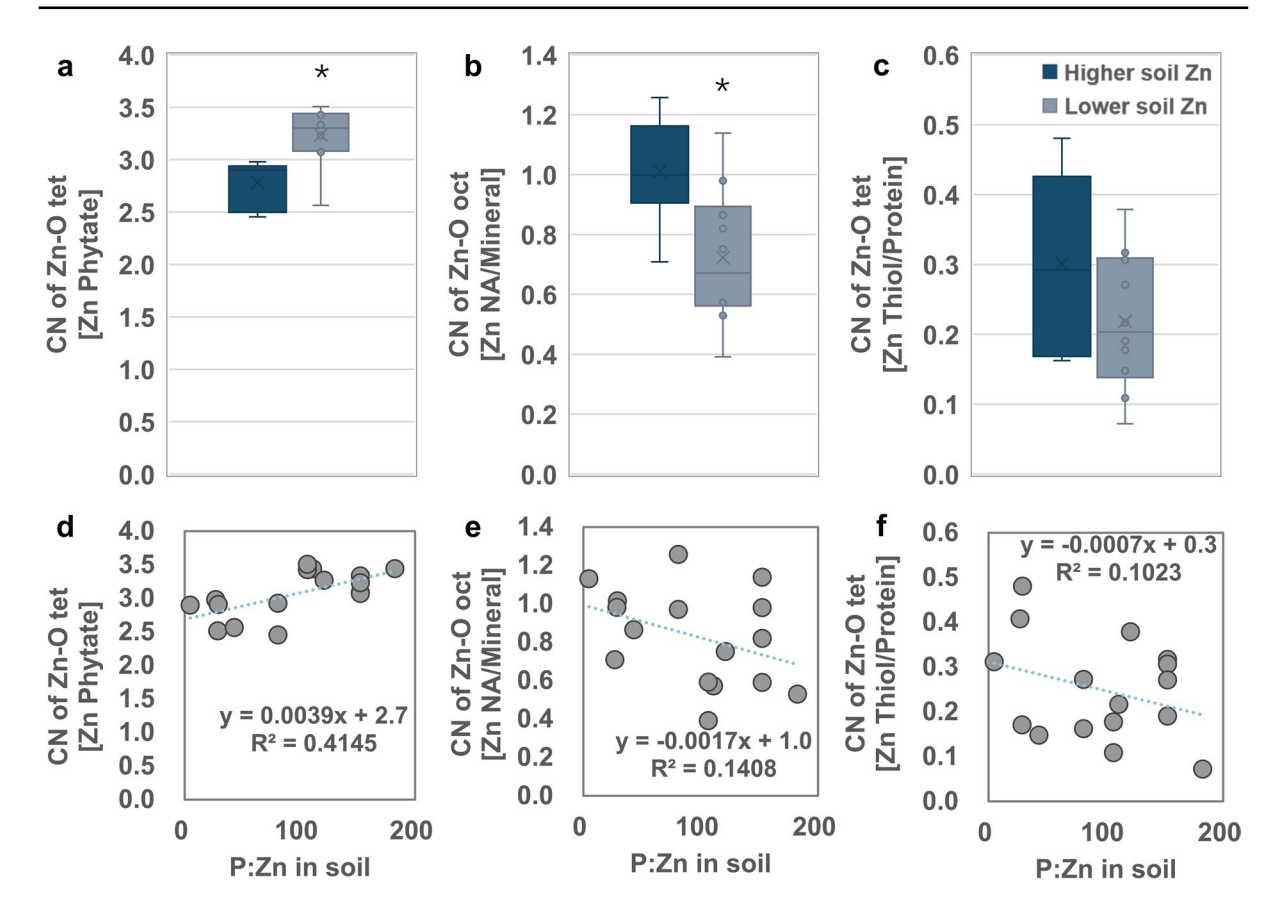


Fig. 4 Coordination numbers (CN) of Zn–O tetrahedral (a), Zn–O octahedral (b) and Zn–S tetrahedral (c) in rice grain grown as a function of soil Zn deficiency and correlation of coordination numbers (CN) of Zn–O tetrahedral (d), Zn–O octahedral (e) and Zn–S tetrahedral (f) with soil P:Zn ratio. Boxplots drawn with the same color borders represent the same kind of Zn species. Dark color-field represents rice grain collected from the soil with high levels of bioavailable Zn (less deficient). Light color-field represents rice grain collected from the soil with lower bioavailable Zn (highly deficient). The box and whisker plot shows the minimum value, first quartile, median, third quartile and maximum value of the

data group. The asterisk (*) indicates that the change between less and more Zn deficiency for the same Zn species is statistically significant (p < 0.05). The change in tetrahedral Zn–O (a), octahedral Zn–O (b) and tetrahedral Zn–S coordination (c) with increasing Zn deficiency indicates that there is an increase in the fraction of Zn phytate complexes, while Zn nicotianamine (NA) complexes or Zn mineral decrease, and Zn thiol complexes similar to those found for Zn bound to thiols in proteins are relatively constant. A good positive linear correlation between tetrahedral Zn–O coordination(d) and the P:Zn ratio in the soil (Pearson correlation coefficient=0.641, p < 0.01) was found

2021) to better understand the connection between Zn phytoaccesibility in soils, and Zn grain concentrations. A holistic approach integrating the dynamics of soil chemical conditions with plant physiology and biochemistry to plant uptake and grain allocation would provide additional insight into this process. Similarly, linking gene expression of relevant genes, or protein activities relevant to Zn acquisition and transport to chemical forms of Zn in the plant would help establish how environmental conditions affect the pathways of Zn uptake and incorporation.

It is useful to contrast the chemical composition and speciation of the Cambodian brown rice samples with rice from other sources. The Chinese black (Market 2), Thai sweet white (Market 3) and Thai red (Market 9) rice grains included in this study also have high levels of Zn phytate, and concentrations of Zn and P are similar to the concentrations observed in Cambodian brown rice samples. Specifically, Market rice 2, Market 3 and Market 9 have 73%, 75% and 79% Zn-phytate based on EXAFS



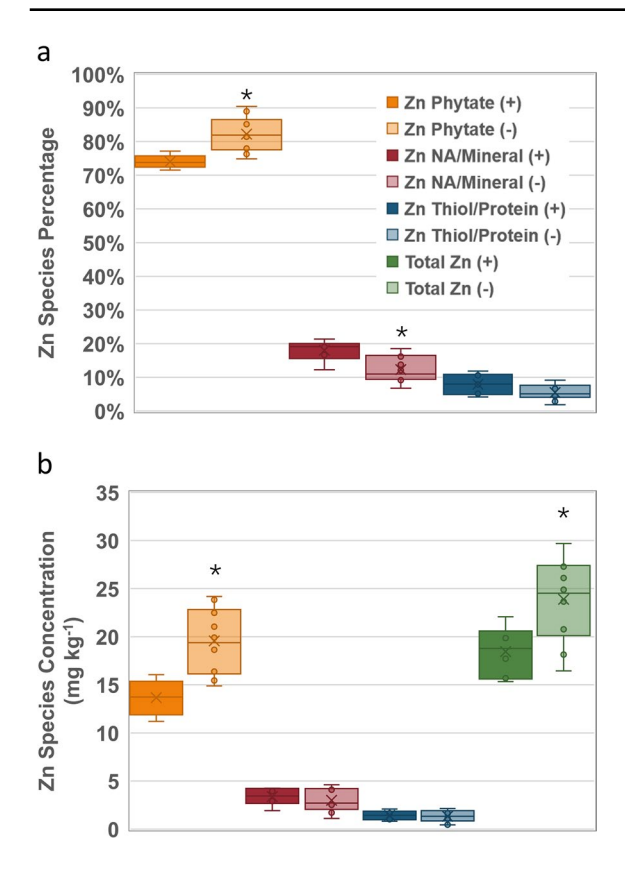


Fig. 5 Boxplot of the fraction (a) and the concentration (b) of Zn phytate, Zn nicotinamide(NA)/mineral and Zn thiol/protein in rice grain grown as a function of soil Zn availability. Boxplots drawn with the same color borders represent the same kind of Zn species. Each Zn species concentration was calculated by multiplying the species percentage with total Zn concentration. Zn Dark color-field (marked with (+)) represents rice grain collected from the soil with higher Zn levels; and light color-field (marked with (-)) represents rice grain collected from soil with lower Zn levels. More Zn phytate is produced under Zn limiting growth conditions. The asterisk (*) indicates that the change between less and more Zn deficiency for the same Zn species is statistically significant (p < 0.05)

spectra, respectively. These Zn-phytate concentrations are similar to the Zn-phytate fractions measured for Cambodian rice grown in soils with higher Zn levels. The similarity even in samples that likely were milled more (removing protein-rich bran and the phytate-rich aleurone) suggests that milling was similar (unlikely) or that these layers did not contain so much Zn as to skew overall results. Speciation within the grain would be useful to confirm this result and could be done with microprobe XRF and XAS.

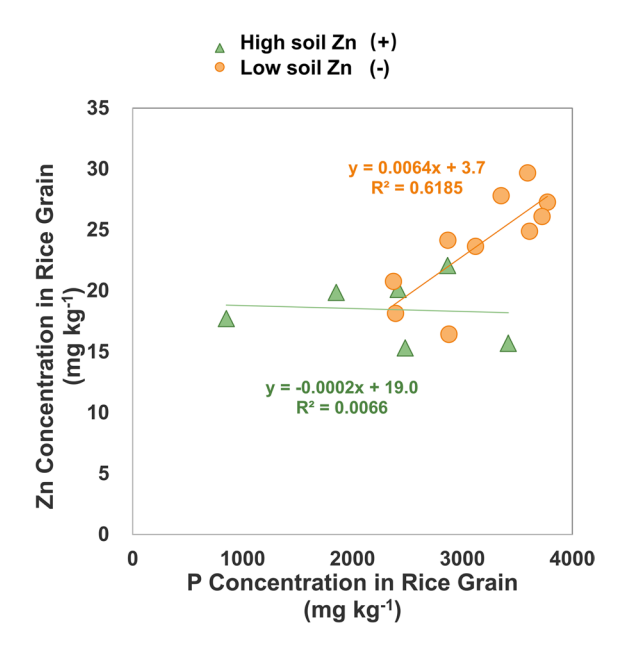


Fig. 6 Total Zn and P concentrations in rice grain as a function of Zn deficiency extent. Green points represent rice grown in soils with higher bioavailable Zn (less limiting values, labeled as high soil Zn(+)) produce rice grain with constant Zn and P content, while orange points represent rice grown in soils with low bioavailable Zn (those with higher levels of Zn deficiency, labeled as low soil Zn(-)) produce rice with higher Zn and P levels. Grain Zn and P levels are positively correlated when rice is grown in less Zn

Conclusion and future perspective

This study is the first to examine the speciation of Zn within the rice grain in situ, and to examine the link between speciation and agricultural Zn deficiency. Overall, we find that Zn concentrations in rice grain are conserved even under severe Zn deficiency, with only minor changes in grain Zn levels as soil levels of Zn increase from very deficient to marginal or adequate levels. We also show that most Zn (70–90%) in rice grain is complexed with phytate, with smaller quantities of Zn-NA/mineral forms, which shows that rice may differ from other small grained cereals. The quantity of Zn-phytate, and thus the quantity of bioavailable Zn, appears to change in response to environmental Zn deficiency (Fig. 5). Although our research does not examine how this occurs, it is likely to involve the increased production of phytate under nutrient deficiency (Wang et al. 2015). The rise in Zn-phytate concentration under Zn nutrient stress



indicates that the Zn species and concentrations of the rice is affected by agricultural deficiencies.

Zn deficiency in soils often lowers rice yields. Our work indicates it also increases the fraction of Zn bound to phytate, potentially making the rice less nutritious because Zn-phytate is less bioavailable (Bohn et al. 2008). Losses in yield and decreased bioavailability of Zn could be significant to susceptible populations that depend on rice as their primary foodstuff, and more broadly across Cambodia. In fact, Zn deficiency and Zn-deficiency related anemia are prevalent across Cambodia (Wieringa et al. 2016), where limited protein consumption makes the population more dependent on nutrient content and availability in the rice that they consume. This is particularly important for subsistence farmers in this study, given that rice represents as much as 80% of their caloric intake. Although rice is not normally considered a Zn-rich food, it is an essential source of Zn in regions like Cambodia where rice consumption is large and consumption of Zn-rich food such as red meat, poultry and shellfish is limited (Gibson 2012). More research should examine Zn uptake from rice, particularly after cooking, to better evaluate whether human uptake is impacted by Zn speciation in the grain.

Last, this study focused on fields with minimally-characterized varieties and genotypes of rice, primarily under conditions (rainfed, with little fertilizer). While these varieties and conditions are common in Cambodia, they differ from many rice growing regions. Further research is needed to determine how rice genotype and variety, which could the plant's response to nutrient limitation, Zn, N, P, K and other fertilizer additions, and flooding extent also can affect Zn speciation more broadly.

Acknowledgements This research is supported by US National Science Foundation (NSF EAR 22-26647), the National Institute of Environmental Health Sciences Superfund Research Program (Grant P42ES033719), the National Science Foundation (NSF) grants EAR 15-21356 and ICR 14-14131, National Institute of Environmental Health Sciences grant ES010349, the Strategic Priority Research Program of Chinese Academy of Sciences (Grant Number XDA20060402), National Natural Science Foundation of China (Grant 41877505), the Guangdong international collaborative grant (2021A0505050001) to Y. Z and an NSF Graduate Research Fellowship to AAN. This research used experimental facilities and beamlines at the Stanford Synchrotron Radiation Lightsource, SLAC National Accelerator Laboratory, supported by the U.S. Department of Energy, Office of Science, Office of Basic Energy Sciences under Contract No. DE-AC02-76SF00515. Data reported in this submission will be available in Columbia Academic Commons.

Author contributions Benjamin C. Bostick planned and designed the research. Benjamin C. Bostick, Yating Shen, Elizabeth Wiita, Athena A. Nghiem and Ezazul Haque performed experiments. Benjamin C. Bostick, Yan Zheng, Elizabeth Wiita, Jingyu Liu, Chheng Y Seng and Kongkea Phan conducted fieldwork. Yating Shen and Benjamin C. Bostick analyzed data. Yating Shen and Benjamin C. Bostick wrote the first manuscript. Yan Zheng, Rachel N. Austin, Elizabeth Wiita, Athena A. Nghiem, Ezazul Haque, Jingyu Liu, Benjamin C. Bostick and Yating Shen review and edit the manuscript.

Funding This work was supported by National Science Foundation (NSF) grants EAR 22-26647, EAR 15–21356 and ICR 14–14131, National Institute of Environmental Health Sciences grants P42ES010349 and P42ES033719, the Strategic Priority Research Program of Chinese Academy of Sciences (Grant Number XDA20060402), National Natural Science Foundation of China (Grant 41877505) and an NSF Graduate Research Fellowship to AAN. This research used experimental facilities and beamlines at the Stanford Synchrotron Radiation Lightsource, SLAC National Accelerator Laboratory, supported by the U.S. Department of Energy, Office of Science, Office of Basic Energy Sciences under Contract No. DE-AC02-76SF00515.

The authors declare that no funds, grants, or other support were received during the preparation of this manuscript.

Data availability Some of the data is available in the Supplementary Information. The datasets generated during and/or analysed during the current study are available from the corresponding author on reasonable request.

Declarations

Competing interests The authors have no relevant financial or non-financial interests to disclose.

References

Abrahams S, Bernstein J (1969) Remeasurement of the structure of hexagonal ZnO. Acta Crystallogr Sect B: Struct Crystallogr Cryst Chem 25(7):1233–1236

Ahmed ZU, Panaullah GM, Gauch H, McCouch SR, Tyagi W, Kabir MS, Duxbury JM (2011) Genotype and environment effects on rice (Oryza sativa L.) grain arsenic concentration in Bangladesh. Plant Soil 338(1):367–382. https://doi.org/10.1007/s11104-010-0551-7

Alloway BJ (2009) Soil factors associated with zinc deficiency in crops and humans. Environ Geochem Health 31(5):537–548. https://doi.org/10.1007/s10653-009-9255-4

Bansal RL, Singh SP, Nayyar VK (1990) The critical zinc deficiency level and response to zinc application of wheat on typic ustochrepts. Exp Agric 26(3):303–306. https://doi.org/10.1017/S0014479700018469

Bewley JD, Bradford K, Hilhorst H, Nonogaki H (2013) Seeds: physiology of development, germination and dormancy (3rd edition), vol 23. Seed Science Research, vol 4. Springer-Verlag New York



624 Plant Soil (2023) 491:605–626

Blair G, Blair N (2014) Nutrient status of cambodian soils, rationalisation of fertiliser recommendations and the challenges ahead for cambodian soil science. Curr Agric Res J 2:05–13. https://doi.org/10.12944/CARJ.2.1.02

- Bohn L, Meyer AS, Rasmussen SK (2008) Phytate: impact on environment and human nutrition. A challenge for molecular breeding. J Zhejiang Univ-Sci B 9(3):165– 191. https://doi.org/10.1631/jzus.B0710640
- Bostick BC, Hansel CM, Fendorf S (2001) Seasonal fluctuations in zinc speciation within a contaminated wetland. Environ Sci Technol 35(19):3823–3829. https://doi.org/ 10.1021/es010549d
- Brown KH, Rivera JA, Bhutta Z, Gibson RS, King JC, Lönnerdal B, Ruel MT, Sandtröm B, Wasantwisut E, Hotz C, Lopez de Romaña D, Peerson JM (2004) International zinc nutrition consultative group (IZINCG) technical document #1. Assessment of the risk of zinc deficiency in populations and options for its control. Food Nutr Bull 25(1, Supplement 2):S94–S203
- Bunquin MAB, Tandy S, Beebout SJ, Schulin R (2017) Influence of soil properties on zinc solubility dynamics under different redox conditions in non-calcareous soils. Pedosphere 27(1):96–105. https://doi.org/10.1016/ S1002-0160(17)60299-6
- Cakmak I (2000) Tansley review No.111 possible roles of zinc in protecting plant cells from damage by reactive oxygen species. New Phytol 146(2):185–205. https:// doi.org/10.1046/j.1469-8137.2000.00630.x
- Cakmak I, Kutman UB (2018) Agronomic biofortification of cereals with zinc: a review. Eur J Soil Sci 69(1):172– 180. https://doi.org/10.1111/ejss.12437
- Cakmak I, Yilmaz A, Kalayci M, Ekiz H, Torun B, Ereno B, Braun H (1996) Zinc deficiency as a critical problem in wheat production in Central Anatolia. Plant Soil 180(2):165–172. https://doi.org/10.1007/bf00015299
- Castillo-Michel HA, Larue C, Pradas del Real AE, Cotte M, Sarret G (2017) Practical review on the use of synchrotron based micro- and nano- X-ray fluorescence mapping and X-ray absorption spectroscopy to investigate the interactions between plants and engineered nanomaterials. Plant Physiol Biochem 110:13–32. https://doi.org/10.1016/j.plaphy.2016.07.018
- Cheng Z, Zheng Y, Mortlock R, van Geen A (2004) Rapid multi-element analysis of groundwater by high-resolution inductively coupled plasma mass spectrometry. Anal Bioanal Chem 379(3):512–518. https://doi.org/10.1007/s00216-004-2618-x
- Christensen AN (1969) The crystal structure of Zn(OH)₂. Acta Chim Scand 23:2016–2020
- Clark-Baldwin K, Tierney DL, Govindaswamy N, Gruff ES, Kim C, Berg J, Koch SA, Penner-Hahn JE (1998) The limitations of X-ray absorption spectroscopy for determining the structure of zinc sites in proteins. When is a tetrathiolate not a tetrathiolate? J Am Chem Soc 120(33):8401–8409
- Clemens S (2014) Zn and Fe biofortification: the right chemical environment for human bioavailability. Plant Sci 225:52–57. https://doi.org/10.1016/j.plantsci.2014.05.014
- Cramer SP, Tench O, Yocum M, George GN (1988) A 13-element ge detector for fluorescence exafs. Nuclear instruments & methods in physics research section

- a-accelerators spectrometers detectors and associated equipment. 266(1-3):586-591. https://doi.org/10.1016/0168-9002(88)90449-4
- Deleon JM, Rehr JJ, Zabinsky SI, Albers RC (1991) Abinitio curved-wave X-ray-absorption fine-structure. Phys Rev B 44(9):4146–4156
- Díaz-Benito P, Banakar R, Rodríguez-Menéndez S, Capell T, Pereiro R, Christou P, Abadía J, Fernández B, Álvarez-Fernández A (2018) Iron and zinc in the embryo and endosperm of rice (Oryza sativa L.) seeds in contrasting 2'-deoxymugineic acid/nicotianamine scenarios. Front Plant Sci 9:1190. https://doi.org/10.3389/fpls.2018.01190
- Dobermann A, Fairhurst T (2000) Zinc deficiency. rice: nutrient disorders and nutrient management. Potash & Phosphate Institute (PPI); Potash & Phosphate Institute of Canada (PPIC). International Rice Research Institute (IRRI):84–89
- Du Laing G, Rinklebe J, Vandecasteele B, Meers E, Tack FMG (2009) Trace metal behaviour in estuarine and riverine floodplain soils and sediments: a review. Sci Total Environ 407(13):3972–3985. https://doi.org/10.1016/j.scitotenv.2008.07.025
- Du Laing G, Vanthuyne DR, Vandecasteele B, Tack FM, Verloo MG (2007) Influence of hydrological regime on pore water metal concentrations in a contaminated sediment-derived soil. Environ Pollut 147(3):615–625. https://doi.org/10.1016/j.envpol.2006.10.004
- EA (2007) UKSHS report No. 1. In: UK Soil and Herbage Pollutant Survey. Environment Agency, Bristol, UK
- Eagling T, Neal AL, McGrath SP, Fairweather-Tait S, Shewry PR, Zhao FJ (2014) Distribution and speciation of iron and zinc in grain of two wheat genotypes. J Agric Food Chem 62(3):708–716. https://doi.org/10.1021/jf403331p
- Effenberger H, Mereiter K, Zemann J (1981) Crystal structure refinements of magnesite, calcite, rhodochrosite, siderite, smithonite, and dolomite, with discussion of some aspects of the stereochemistry of calcite type carbonates. Z Kristallogr-Cryst Mater 156(1–4):233–244
- Fanselow R, Sobstel M, Błachucki W, Szlachetko J (2022) Performance of a laboratory von Hámos type x-ray spectrometer in x-ray absorption spectroscopy study on 3d group metals. X-Ray Spectrom. https://doi.org/10.1002/xrs.3317
- Farooq M, Wahid A, Siddique KHM (2012) Micronutrient application through seed treatments a review. J Soil Sci Plant Nutr 12(1):125–142. https://doi.org/10.4067/s0718-95162012000100011
- Gao X, Hoffland E, Stomph T, Grant CA, Zou C (2012) Improving zinc bioavailability in transition from flooded to aerobic rice. A Review. Agron Sustain Dev 32(2):465– 478. https://doi.org/10.1007/s13593-011-0053-x
- Gibson RS (2012) A historical review of progress in the assessment of dietary zinc intake as an indicator of population zinc status. Adv Nutr 3(6):772–782. https://doi.org/10.3945/an.112.002287
- Grafe M, Donner E, Collins RN, Lombi E (2014) Speciation of metal(loid)s in environmental samples by X-ray absorption spectroscopy: a critical review. Anal Chim Acta 822:1–22. https://doi.org/10.1016/j.aca.2014.02.044
- Graham RD, Knez M, Welch RM (2012) Chapter one how much nutritional iron deficiency in humans globally is due to an underlying zinc deficiency? In: Sparks DL



- (ed) Advances in Agronomy. Academic Press, vol 115, pp 1–40. https://doi.org/10.1016/B978-0-12-394276-0. 00001-9
- GRiSP (Global Rice Science Partnership). (2013) Rice almanac, 4th edn. International Rice Research Institute, Los Baños (Philippines), p 283
- Guilherme Buzanich A (2022) Recent developments of X-ray absorption spectroscopy as analytical tool for biological and biomedical applications. X-Ray Spectrom 51(3):294–303. https://doi.org/10.1002/xrs.3254
- Impa SM, Johnson-Beebout SE (2012) Mitigating zinc deficiency and achieving high grain Zn in rice through integration of soil chemistry and plant physiology research. Plant Soil 361(1):3–41. https://doi.org/10.1007/ s11104-012-1315-3
- Iwai T, Takahashi M, Oda K, Terada Y, Yoshida KT (2012) Dynamic changes in the distribution of minerals in relation to phytic acid accumulation during rice seed development. Plant Physiol 160(4):2007–2014. https://doi.org/10. 1104/pp.112.206573
- Johnson-Beebout SE, Lauren JG, Duxbury JM (2009) Immobilization of zinc fertilizer in flooded soils monitored by adapted DTPA soil test. Commun Soil Sci Plant Anal 40(11–12):1842–1861
- Jones DL, Cross P, Withers PJA, DeLuca TH, Robinson DA, Quilliam RS, Harris IM, Chadwick DR, Edwards-Jones G (2013) Review: nutrient stripping: the global disparity between food security and soil nutrient stocks. J Appl Ecol 50(4):851–862. https://doi.org/10.1111/1365-2664. 12089
- Joshi AK, Crossa J, Arun B, Chand R, Trethowan R, Vargas M, Ortiz-Monasterio I (2010) Genotypexenvironment interaction for zinc and iron concentration of wheat grain in eastern Gangetic plains of India. Field Crop Res 116(3):268–277. https://doi.org/10.1016/j.fcr.2010.01.004
- Ketenoglu D (2022) A general overview and comparative interpretation on element-specific X-ray spectroscopy techniques: XPS, XAS, and XRS. X-Ray Spectrom 51(5– 6):422–443. https://doi.org/10.1002/xrs.3299
- Khampuang K, Rerkasem B, Lordkaew S, Prom-u-thai C (2021) Nitrogen fertilizer increases grain zinc along with yield in high yield rice varieties initially low in grain zinc concentration. Plant Soil 467(1–2):239–252. https://doi.org/10.1007/s11104-021-05090-w
- Kirk G (2004) The biogeochemistry of submerged soils. Wiley, New York, p 304
- Kisi EH, Elcombe MM (1989) *u* parameters for the wurtzite structure of ZnS and ZnO using powder neutron diffraction. Acta Crystallogr C 45(12):1867–1870
- Lemmens E, De Brier N, Spiers KM, Ryan C, Garrevoet J, Falkenberg G, Goos P, Smolders E, Delcour JA (2018) The impact of steeping, germination and hydrothermal processing of wheat (Triticum aestivum L.) grains on phytate hydrolysis and the distribution, speciation and bio-accessibility of iron and zinc elements. Food Chem 264:367–376. https://doi.org/10.1016/j.foodchem.2018.04.125
- Liang J, Li Z, Tsuji K, Nakano K, Nout MJR, Hamer RJ (2008) Milling characteristics and distribution of phytic acid and zinc in long-, medium- and short-grain rice. J Cereal Sci 48(1):83–91. https://doi.org/10.1016/j.jcs.2007.08.003

- Liu ZH, Wang HY, Wang XE, Zhang GP, Chen PD, Liu DJ (2007) Phytase activity, phytate, iron, and zinc contents in wheat pearling fractions and their variation across production locations. J Cereal Sci 45(3):319–326. https://doi.org/ 10.1016/j.jcs.2006.10.004
- Lv HH, Ding JL, Zhang L, Wang C, Cai HM (2022) Zinc application facilitates the turnover of organic phosphorus in rice rhizosphere soil by modifying microbial communities. Plant Soil. https://doi.org/10.1007/ s11104-022-05810-w
- Machado AS, de Sá Silva AS, de Araújo OMO, Santos RS, Leitão RG, dos Anjos MJ, de Oliveira DF, Lopes RT (2023) Analysis of the quality of industrialized coffee powder using the techniques of computed microtomography and x-ray fluorescence. X-Ray Spectrom. https://doi. org/10.1002/xrs.3326
- Mayhew L, Webb S, Templeton A (2011) Microscale imaging and identification of Fe speciation and distribution during fluid–mineral reactions under highly reducing conditions. Environ Sci Technol 45(10):4468–4474
- Neue HU, Quijano C, Senadhira D, Setter T (1998) Strategies for dealing with micronutrient disorders and salinity in lowland rice systems. Field Crop Res 56(1):139–155. https://doi.org/10.1016/S0378-4290(97)00125-1
- Newville M (2001) EXAFS analysis using FEFF and FEFFIT. J Synchrotron Radiat 8:96–100. https://doi.org/10.1107/ s0909049500016290
- O'day PA, Carroll SA, Waychunas GA (1998) Rock-water interactions controlling zinc, cadmium, and lead concentrations in surface waters and sediments, US Tri-State mining district. 1. Molecular identification using X-ray absorption spectroscopy. Environ Sci Technol 32(7):943–955
- Persson DP, de Bang TC, Pedas PR, Kutman UB, Cakmak I, Andersen B, Finnie C, Schjoerring JK, Husted S (2016) Molecular speciation and tissue compartmentation of zinc in durum wheat grains with contrasting nutritional status. New Phytol 211(4):1255–1265. https://doi.org/10.1111/ nph.13989
- Persson DP, Hansen TH, Laursen KH, Schjoerring JK, Husted S (2009) Simultaneous iron, zinc, sulfur and phosphorus speciation analysis of barley grain tissues using SEC-ICP-MS and IP-ICP-MS. Metallomics 1(5):418–426. https://doi.org/10.1039/B905688B
- Pfeiffer WH, McClafferty B (2007) Harvestplus: breeding crops for better nutrition. Crop Sci 47(Supplement_3):S-88-S-105. https://doi.org/10.2135/cropsci2007.09.0020I PBS
- Phan K, Phan S, Heng S, Huoy L, Kim K-W (2014) Assessing arsenic intake from groundwater and rice by residents in Prey Veng province, Cambodia. Environ Pollut 185:84–89
- Prasad AS (2014) Impact of the discovery of human zinc deficiency on health. J Trace Elem Med Biol 28(4):357–363. https://doi.org/10.1016/j.jtemb.2014.09.002
- Prentice AM, Gershwin ME, Schaible UE, Keusch GT, Victora CG, Gordon JI (2008) New challenges in studying nutrition-disease interactions in the developing world. J Clin Investig 118(4):1322–1329. https://doi.org/10.1172/JCI34034
- Raboy V (2009) Approaches and challenges to engineering seed phytate and total phosphorus. Plant Sci 177(4):281–296. https://doi.org/10.1016/j.plantsci.2009.06.012



626 Plant Soil (2023) 491:605–626

Ravindran V, Ravindran G, Sivalogan S (1994) Total and phytate phosphorus contents of various foods and feed-stuffs of plant-origin. Food Chem 50(2):133–136. https://doi.org/10.1016/0308-8146(94)90109-0

- Rotich NK, Gatari MJ, Kareru P, Boman J (2023) Essential trace elements in the African spider plant (Cleome gynandra). A case study in Molo Ward, Nakuru, Kenya. X-Ray Spectrom 52(2):83–89. https://doi.org/10.1002/xrs.3323
- Rutkowska B, Szulc W, Bomze K (2013) Plant availability of zinc in differentiated soil conditions. Fresenius Environ Bull 22(9):2542–2546
- Sandberg A-S, Andersson H (1988) Effect of dietary phytase on the digestion of phytate in the stomach and small intestine of humans. J Nutr 118(4):469–473
- Sar S, Gilbert RG, Marks GC (2012) Household rice choice and consumption behavior across agro-climatic zones of cambodia. J Hunger Environ Nutr 7(2–3):333–346. https://doi.org/10.1080/19320248.2012.707107
- Sarret G, Saumitou-Laprade P, Bert V, Proux O, Hazemann J-L, Traverse A, Marcus MA, Manceau A (2002) Forms of zinc accumulated in the hyperaccumulatorArabidopsis halleri. Plant Physiol 130(4):1815–1826
- Sarret G, Vangronsveld J, Manceau A, Musso M, D'Haen J, Menthonnex J-J, Hazemann J-L (2001) Accumulation forms of Zn and Pb in Phaseolus vulgaris in the presence and absence of EDTA. Environ Sci Technol 35(13):2854– 2859. https://doi.org/10.1021/es000219d
- Seck PA, Diagne A, Mohanty S, Wopereis MCS (2012) Crops that feed the world 7: rice. Food Security 4(1):7–24. https://doi.org/10.1007/s12571-012-0168-1
- Seyfferth AL, McCurdy S, Schaefer MV, Fendorf S (2014) Arsenic concentrations in paddy soil and rice and health implications for major rice-growing regions of Cambodia. Environ Sci Technol 48(9):4699–4706
- Sillanpää M (1982) Micronutrients and the nutrient status of soils: a global study. Food and Agriculture Organization of the United Nations, Rome
- Stewart CP, Dewey KG, Ashorn P (2010) The undernutrition epidemic: an urgent health priority. Lancet 375(9711):282. https://doi.org/10.1016/S0140-6736(10)60132-8
- Takahashi M, Nozoye T, Kitajima N, Fukuda N, Hokura A, Terada Y, Nakai I, Ishimaru Y, Kobayashi T, Nakanishi H, Nishizawa NK (2009) In vivo analysis of metal distribution and expression of metal transporters in rice seed during germination process by microarray and X-ray Fluorescence Imaging of Fe, Zn, Mn, and Cu. Plant Soil 325(1):39–51. https://doi.org/10.1007/s11104-009-0045-7
- Thomas SA, Mishra B, Myneni SCB (2019) High energy resolution-X-ray absorption near edge structure spectroscopy reveals zn ligation in whole cell bacteria. J Phys Chem Lett 10(10):2585–2592. https://doi.org/10.1021/acs.jpclett.9b01186

- Trampczynska A, Küpper H, Meyer-Klaucke W, Schmidt H, Clemens S (2010) Nicotianamine forms complexes with Zn (II) in vivo. Metallomics 2(1):57–66
- Wang Z, Liu Q, Pan F, Yuan L, Yin X (2015) Effects of increasing rates of zinc fertilization on phytic acid and phytic acid/zinc molar ratio in zinc bio-fortified wheat. Field Crop Res 184:58–64. https://doi.org/10.1016/j.fcr. 2015.09.007
- Webb SM (2005) SIXPack a graphical user interface for XAS analysis using IFEFFIT. Phys Scr:1011. https://doi.org/10.1238/physica.topical.115a01011
- Webb SM (2011) The microanalysis toolkit: X-ray fluorescence image processing software. AIP Conf Proc 1365(1):196– 199. https://doi.org/10.1063/1.3625338
- Wessells KR, Brown KH (2012) Estimating the global prevalence of zinc deficiency: results based on zinc availability in national food supplies and the prevalence of stunting. PLoS ONE 7(11):e50568
- Wieringa FT, Dahl M, Chamnan C, Poirot E, Kuong K, Sophonneary P, Sinuon M, Greuffeille V, Hong R, Berger J (2016) The high prevalence of anemia in Cambodian children and women cannot be satisfactorily explained by nutritional deficiencies or hemoglobin disorders. Nutrients 8(6):348
- Wisawapipat W, Janlaksana Y, Christl I (2017) Zinc solubility in tropical paddy soils: a multi-chemical extraction technique study. Geoderma 301:1–10. https://doi.org/10.1016/j.geoderma.2017.04.002
- Wissuwa M, Ismail AM, Graham RD (2008) Rice grain zinc concentrations as affected by genotype, native soil-zinc availability, and zinc fertilization. Plant Soil 306(1–2):37–48. https://doi.org/10.1007/s11104-007-9368-4
- Zabinsky SI, Rehr JJ, Ankudinov A, Albers RC, Eller MJ (1995) Multiple-scattering calculations of X-ray-absorption spectra. Phys Rev B 52(4):2995–3009. https://doi.org/10.1103/PhysRevB.52.2995

Publisher's note Springer Nature remains neutral with regard to jurisdictional claims in published maps and institutional affiliations.

Springer Nature or its licensor (e.g. a society or other partner) holds exclusive rights to this article under a publishing agreement with the author(s) or other rightsholder(s); author self-archiving of the accepted manuscript version of this article is solely governed by the terms of such publishing agreement and applicable law.

